become a focus of research. Accumulating evidence indicates that ROS induce neoplasia by mutating nuclear and mitochondrial DNA (Ishii et al., 2005) or by signaling a pseudohypoxic condition by stabilization of the HIF-1α under normoxic conditions (Guzy et al., 2008). To date, the FAD site is proposed as the ROS producing site in complex II, based on studies done on *Escherichia coli* (Messner and Imlay, 2002), whereas the quinone binding site is proposed as the site of ROS production based on studies in *Saccharomyces cerevisiae* (Guo and Lemire, 2003; Szeto et al., 2007).

In adult worms of the parasitic helminth *Ascaris suum*, complex II functions as the terminal oxidase of the anaerobic respiratory chain and catalyzes fumarate reduction (quinol-fumarate reductase; QFR; Kita et al., 2007). Consistent with its physiological function, it shows high fumarate reductase (FRD) activity when the water-soluble dye methyl viologen is used as an artificial electron donor (Amino et al., 2003). Although the adult enzyme shows high FRD activity, the amino acid sequences of all four of its subunits are more similar to the mitochondrial SQR than to the bacterial QFR (Amino et al., 2000; Amino et al., 2003; Kuramochi et al., 1994; Saruta et al., 1995; Saruta et al., 1996). Moreover, the amino acid residues in the FAD binding site and the active site in the catalytic domain as well as the quinone binding site (Q site) are similar to the mitochondrial SQR. In addition, it shows high SQR activity *in vitro* (Iwata et al., 2008; Kita et al., 2002).

During a study of complex II in adult *A. suum*, we found a significant degree of succinate–cytochrome *c* reductase activity in purified *A. suum* adult complex II, even though the preparation did not contain complex III (quinol-cytochrome *c* reductase) (Takamiya et al., 1986). This result raised the possibility that significant electron leak occurred from adult complex II. In the present study, in attempting to verify this possibility, we investigated succinate-dependent ROS production from the parasite's mitochondria. Analysis of submitochondrial particles for superoxide (O_2^-) production using superoxide dismutase inhibitable acetylated cytochrome *c* reduction, and hydrogen peroxide production using catalase inhibitable amplex red oxidation, in the presence and absence of respiratory chain inhibitors, showed the contribution from both the FAD site and Q site of complex II to produce O_2^- and H_2O_2 when succinate is oxidized under aerobic conditions. Considering the conservation of amino acid residues critical for the enzyme reaction between *A. suum* complex II and mitochondrial SQR, our results show that ROS are produced from more than one site in mitochondrial complex II, linked with subtle differences in the amino acid sequences of the enzyme complex.

2. Materials and methods

2.1. Chemicals

Amplex red was obtained from Molecular probes (Eugene, Oregon). Acetylated cytochrome *c*, superoxide dismutase (bovine and *E. coli*), and horseradish peroxidase were from Sigma Chemical Company, USA. Catalase was from Wako, Japan. Atpenin A5 was from Alexis Biochemicals, Switzerland.

2.2. Submitochondrial particles (SMPs)

SMPs were prepared from frozen muscles of *A. suum* adult female worms by the modified method of Matsuno-Yagi and Hatefi (1985). During preparation of mitochondria, Chappell Perry buffer (100 mM KCl, 50 mM Tris–HCl, 1 mM ATP, 5 mM $MgCl_2$ and 1 mM EDTA, pH 7.4) containing 10 mM sodium malonate was used (Yamashita et al., 2004). Mitochondria were subjected to sonication four times for 30 s with 1.5-min intervals (Branson 450 D, Japan) in the same buffer containing 1 mM sodium malonate and $MgCl_2$ and $MnCl_2$ at a final concentration of 10 mM. In addition, the SMP were washed three times in Chappell Perry buffer with 1 mM sodium malonate buffer to remove the ROS scavenging molecules and stored at −80 °C. Mitochondria from L_3 larvae were prepared as previously described (Amino et al., 2003). SMPs were prepared from frozen mitochondria of *A. suum* L_3 larvae by sonicating three times for 30 s with 1.5-min intervals in a water bath sonifier (Sibata Su-25, Model SSC-350H, Japan). They were washed as described in adult SMP preparation and stored at −80 °C. The protein concentration in the SMP samples was estimated by Lowry's method (Lowry et al., 1951), using bovine serum albumin as the standard.

2.3. Superoxide generation assay

The superoxide radical generation rate was assayed using superoxide dismutase (SOD) inhibitable acetylated cytochrome *c* reduction (Azzi et al., 1975; Imlay and Fridovich, 1991; Zhao et al., 2006). The assay was performed in 50 mM potassium phosphate buffer (pH 7.4) containing, 0.25 M sucrose and 1 mM $MgCl_2$ at 25 °C in the presence of 25 μM acetyl cytochrome *c* and 15 μg/ml SMP in a total reaction mixture of 1 ml. After pre-incubating the mixture for 2 min, the reaction was started by adding 0.75 mM sodium succinate or 50 μM NADH. A parallel reaction was run with an additional 30 U/ml superoxide dismutase. The reduction of acetylated cytochrome *c* was monitored spectrophotometrically as the difference in absorbance at 550–540 nm and calculated using the difference in extinction coefficients of ferrocytochrome *c* and ferricytochrome *c*, $\varepsilon^{550-540} = 19\ mM^{-1}\ cm^{-1}$. Non-specific reduction of acetyl cytochrome *c* was excluded by subtracting the amount of cytochrome *c* reduced in the presence of SOD from that in the absence of SOD.

2.4. H_2O_2 generation assay

Oxidation of amplex red (10-acetyl-3,7-dihydroxyphenoxazine) to resorufin was used to assay the H_2O_2 generation rate (Chen et al., 2003; Mohanty et al., 1997; Shinjyo and Kita, 2007). The assay was performed in 50 mM potassium phosphate buffer (pH 7.4) containing, 0.25 M sucrose and 1 mM $MgCl_2$, 50 μmol amplex red, 0.2 U/ml horseradish peroxidase, 15 μg/ml SMP, and 0.75 mM sodium succinate or 50 μM NADH in a total reaction mixture of 1.0 ml maintained at 25 °C. A parallel reaction was run with an additional 1000 U/ml catalase. The resorufin formation rate was monitored spectrophotometrically at 571 nm. The H_2O_2 generation rate was calculated by using a standard curve. Specificity of the reaction was obtained by subtracting the amount of H_2O_2 produced in the presence of catalase from that in the absence of catalase.

In *A. suum* adult SMP, both the O_2^- and H_2O_2 generation assays were also performed in the presence of 10 mM sodium malonate which blocks the dicarboxylate-binding site of complex II; 400 nM atpenin A5, which blocks the Q site of complex II; and 40 nM quinazoline, which blocks the Q site of complex I. In *A. suum* L_3 larval SMP, 10 μM antimycin A (Qi site inhibitor of complex III), 5 μM stigmatellin (Qo site inhibitor of complex III), 5 μM rotenone (Q site inhibitor of complex I) were also employed in the assays. All these inhibitors at the above-mentioned concentrations reduced more than 85% of the corresponding activities.

2.5. Statistical analysis

All the assays were performed in triplicate and the results were expressed as means ± SEM. O_2^- or H_2O_2 production from a particular organism with a given substrate was compared between different experimental conditions using one-way analysis of

variance followed by the Tukey test. The level of significance was $p < 0.05$.

3. Results

3.1. Complex II is the main ROS producing site in the respiratory chain of adult A. suum

Since the presence of antioxidant molecules in the mitochondria interfered with accurate ROS detection, inside-out submitochondrial particles were prepared and washed to eliminate the antioxidant molecules. As shown in Figs. 1a and 1b, substantial production of O_2^- and H_2O_2 was observed from the submitochondrial particles of *A. suum* adults and L_3 larvae. Then, a series of respiratory chain inhibitors in combination with the respiratory substrates were employed in the assays in order to localize the site of ROS production. Quinazoline is a Q site inhibitor of *A. suum* adult complex I (Yamashita et al., 2004) (Fig. 2a). During succinate oxidation, i.e., electron entry into the respiratory chain from complex II, the addition of quinazoline inhibits the reverse flow of electrons into complex I from the quinone pool. As shown in Table 1, quinazoline inhibition did not show a significant effect on succinate-dependent O_2^- production. This result indicates that the contribution of complex I for succinate-dependent ROS production in *A. suum* adult worms is not significant. Since complex III and IV activities are not found in the respiratory chain of adult *A. suum*, the only significant source of O_2^- in its submitochondrial particles must be complex II. Moreover, the addition of quinazoline in the reaction mixture during NADH oxidation, i.e., electron entry from complex I, resulted in 95% suppression of the O_2^- production rate (Table 1) suggesting the possibility of either the Q site of complex I or a redox center/centers in complex II to be the major O_2^- production sites. In order to assess the contribution of the Q site in complex I for O_2^- production, atpenin A5, which inhibits the SQR activity of complex II completely in *A. suum* (Miyadera et al., 2003) (Fig. 2a), was employed. The NADH-dependent O_2^- production rate observed in the presence of atpenin A5 was not significantly different from that in the presence of quinazoline (Table 1), indicating that the Q site of complex I does not contribute to NADH-dependent O_2^- production significantly. The effect of inhibitors on succinate- and NADH-dependent hydrogen peroxide production rates also showed a similar pattern to that of O_2^- (data not shown). Collectively, the above data provide clear evidence to show that complex II is the main ROS producing site in the respiratory chain of *A. suum* adult worms.

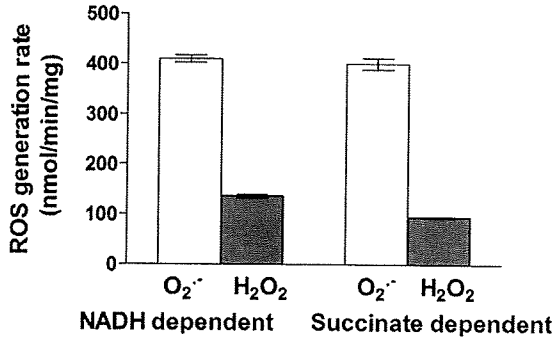

Fig. 1a. Superoxide and hydrogen peroxide generation by SMP of adult *A. suum* worms oxidizing 0.75 mM succinate or 50 μM NADH. Superoxide production was measured as superoxide dismutase inhibitable reduction of acetylated cytochrome *c*, and hydrogen peroxide production was measured as catalase inhibitable oxidation of amplex red as described in Section 2. Results are expressed as means ± SEM of triplicate measurements from three different pools of submitochondrial particles.

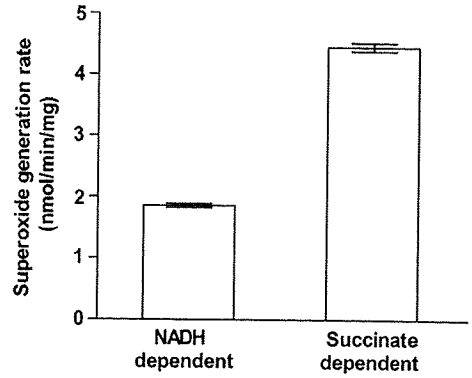

Fig. 1b. Superoxide generation by SMP of *A. suum* L_3 larvae oxidizing 0.5 mM succinate or 50 μM NADH. Superoxide production was measured as superoxide dismutase inhibitable reduction of acetylated cytochrome *c* as described in Section 2. Results are expressed as means ± SEM of triplicate measurements from a single pool of submitochondrial particles. No detectable level of hydrogen peroxide was produced when measured as catalase inhibitable oxidation of amplex red as described in Section 2.

Table 1
Superoxide production from submitochondrial particles of *A. suum* adult worms oxidizing 0.5 mM succinate and 50 μM NADH in the presence of respiratory chain inhibitors. Superoxide production was determined as superoxide dismutase inhibitable reduction of acetylated cytochrome *c* as described in Secton 2. Values are given as nmol/min/mg of protein and expressed as means ± SEM from triplicate measurements on one pool of submitochondrial particles. The decrease of superoxide production (%) in the presence of the inhibitor compared to that in the absence of the inhibitor is given in parentheses.

	Succinate	NADH
No inhibitor	400 ± 11	410 ± 7.75
Quinazoline (40 nM)	359 ± 12 (−10%)	21.1 ± 1.01[b] (−95%)
Atpenin A5 (400 nM)	246 ± 5[a] (−38%)	24.0 ± 0.58[b] (−94%)
Malonate (10 mM)	ND[d]	67.8 ± 4.21[c] (−83%)

[a,b,c] Significantly different from the measurement without an inhibitor. $p < 0.05$.
There was no significant difference between [b]$p < 0.05$.
There was a significant difference between [b]and [c]$p < 0.05$.
[d] ND: not detectable.

3.2. ROS production from the respiratory chain of A. suum L_3 larvae

In *A. suum* L_3 larvae, components of the respiratory chain are similar to those of mammalian mitochondria (Kita and Takamiya, 2002), and complex II serves as SQR. Since the subunit composition of L_3 larvae complex II is different from that of the adult worm (Amino et al., 2000; Amino et al., 2003), succinate- and NADH-dependent ROS production from the SMP of L_3 larvae was also measured in the presence of 5 μM rotenone (Q site inhibitor of complex I), 10 μM antimycin A (Qi site inhibitor of complex III), 5 μM stigmatellin (Qo site inhibitor of complex III), and 10 mM NaN_3 (complex IV inhibitor). In L_3 larvae, the succinate-dependent O_2^- production rate was not significantly affected by the addition of these inhibitors (Table 2). This suggests that complexes I, III, and IV of the L_3 larval respiratory chain do not contribute to O_2^- production during succinate oxidation. Yet, O_2^- production during succinate oxidation was almost completely inhibited by 10 mM malonate and 14% inhibited by atpenin A5. Taken together, these data indicate that complex II is the main succinate-dependent ROS producing site in the submitochondrial particles of *A. suum* L_3 larvae, as is the case for adult worms. On the other hand, malonate and atpenin A5 did not have any effect on NADH-dependent O_2^- production, whereas rotenone significantly increased it. O_2^- production rates in the presence of antimycin A and stigmatellin or NaN_3 were similar to that in the presence of rotenone. These

Table 2
Superoxide production from submitochondrial particles of *A. suum* L_3 larvae oxidizing 0.5 mM succinate or 50 μM NADH in the presence of respiratory chain inhibitors. Superoxide production was determined as superoxide dismutase inhibitable reduction of acetylated cytochrome *c* as described in Section 2. Values are given as nmol/min/mg of protein expressed as means ± SEM from triplicate measurements on one pool of submitochondrial particles. The change of superoxide production (%) in the presence of the inhibitor compared to that in the absence of the inhibitor is given in parentheses.

	Succinate	NADH
No inhibitor	4.45 ± 0.07	1.86 ± 0.03
Rotenone (5 μM)	4.42 ± 0.03 (−0.7%)	2.29 ± 0.07[b] (+23%)
AntimycinA (10 μM)	4.56 ± 0.07 (+3%)	1.62 ± 0.07 (−13%)
Antimycin A (10 μM) + Stigmatellin (5 μM)	4.81 ± 0.03 (+8%)	2.53 ± 0.03[b] (+36%)
NaN_3 (10 mM)	4.87 ± 0 (+9%)	2.63 ± 0.04[b] (+41%)
Malonate (10 mM)	ND[d]	1.62 ± 0.13 (−13%)
Atpenin A5 (400 nM)	3.85 ± 0.07[a] (−14%)	1.82 ± 0.01 (−2%)

[a,b] Significantly different from the measurement without an inhibitor. $p < 0.05$. There was no significant difference among [b] $p < 0.05$.
[d] ND: not detectable.

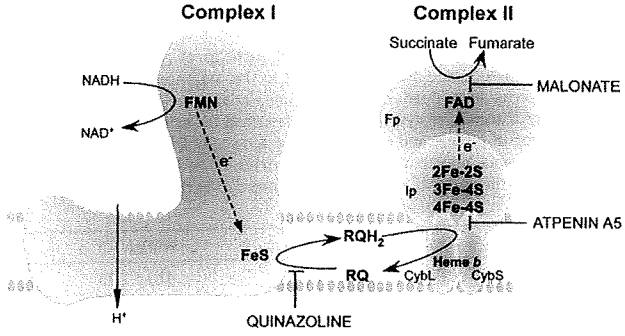

Fig. 2a. Schematic representation of the flow of electrons and the sites of action of inhibitors in the respiratory chain complexes of *A. suum* adult worms.

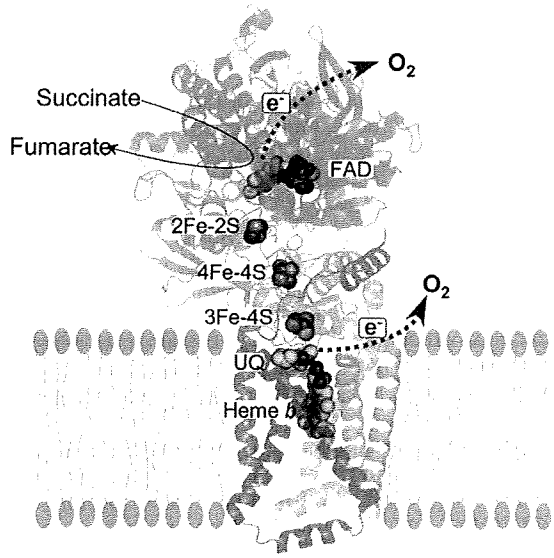

Fig. 2b. Ribbon model of mitochondrial complex II of *S. scrofa* (pdb1ZOY) showing the potential reactive oxygen species production sites identified in *A. suum*. Fp, Ip, CybL and CybS subunits are shown in green, blue, red and orange respectively. The redox centers, FAD, iron-sulfur clusters and heme *b* are as labeled in the figure. Rhodoquinone is supposed to bind to the position of ubiquinone.

observations imply that a redox center in complex I upstream to its Q site is the source of NADH-dependent O_2^- in L_3 larvae. Blocking of complexes III or IV leads to accumulation of electrons at complex I, enhancing the O_2^- production from this site in a similar manner to rotenone. Interestingly, unlike in many mammalian tissues, blocking of the Qi site in complex III did not increase the O_2^- production by submitochondrial particles of L_3 larvae. A quantitative comparison of ROS production between complexes I and II in *A. suum* L_3 larvae showed that the succinate-dependent O_2^- production from complex II is 3-fold higher than NADH-dependent O_2^- production from complex I (Table 2).

3.3. ROS are produced from more than one site in A. suum mitochondrial complex II

In *E. coli*, the flavin of complex IIs is considered to be the source of ROS (Messner and Imlay, 2002). In these enzymes, succinate-dependent ROS production is at a maximum at a lower succinate concentration (at about 1 mM), and at higher succinate concentrations (around 50–100 mM), it is completely inhibited. Hence, excess succinate is suggested to suppress ROS production by hindering the access of oxygen to FAD, thus preventing its autoxidation. When we measured the succinate-dependent ROS production in *A. suum* SMP, it increased with substrate concentration and was highest at 0.5–1 mM succinate in both adults and L_3 larvae (Fig. 3) and gradually decreased along with increasing succinate concentrations. This finding is in accordance with the findings on *E. coli* complex IIs by Messner and Imlay (2002).

However, the percentage of inhibition in ROS production at ⩾100 mM succinate in *A. suum* complex II was only 80%, with 20% always remaining. Further, as shown in Table 1, NADH-dependent O_2^- production was only 83% suppressed by the addition of 10 mM malonate into the reaction mixture. Since malonate is a succinate analogue, which is also known to bind in close proximity to the FAD site in mitochondrial complex II (Huang et al., 2006), it is likely to block the interaction between *A. suum* FAD and oxygen in a manner similar to that in *E. coli* complex IIs, thus decreasing the O_2^- production from the FAD site. Such residual ROS production observed even after complete blocking of the FAD site with succinate or malonate suggests another site for ROS production, in addition to FAD.

The Q site is the other candidate for a potential source of ROS in complex II as reported by Guo and Lemire (2003), and Zhao et al.,

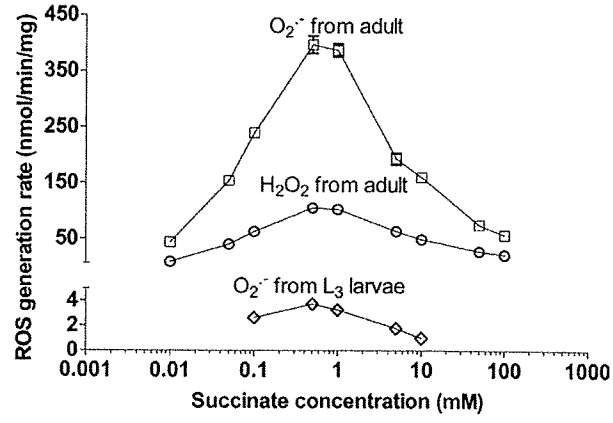

Fig. 3. Effect of succinate concentration on ROS production from *A. suum* SMP. Reaction media for superoxide and hydrogen peroxide measurements were prepared as described in Section 2. Reactions were initiated by addition of succinate at a concentration range of 0.01–100 mM. Points indicate means ± SEM in triplicate measurements from three different pools of SMPs in adult worms and from a single pool in L_3 larvae.

2006. To determine the contribution of the Q site of *A. suum* complex II to ROS production, we analyzed its ROS production in the presence of 400 nM atpenin A5, which inhibits the Q site of complex II completely. O_2^- production from complex II of *A. suum* adult worms with 0.75 mM succinate was decreased 38% in the presence of atpenin A5 (Table 1). In L_3 larvae, it was decreased approximately 14% (Table 2). This observation indicates that binding of atpenin A5 results in reduction in ROS production from *A. suum* complex IIs. In another ROS producing system, xanthine oxidase/hypoxanthine, atpenin A5 interfered with neither ROS production nor detection (data not shown), suggesting that atpenin A5 does not serve as a radical scavenger. Thus, it appears that electrons leak to oxygen from the Q site also during succinate oxidation. Atpenin A5 may inhibit either binding and/or reduction of quinone, thus preventing electron flow in the Q site and inhibiting ROS production.

4. Discussion

Mitochondrial respiratory chain is a significant source of cellular ROS. Impairment of the respiratory chain complexes is known to increase the cellular ROS production (Indo et al., 2007). Historically, complexes I and III are considered as the two major sites of superoxide and hydrogen peroxide production in the respiratory chain (Jezek and Hlavata, 2005; Murphy, 2009; St-Pierre et al., 2002). Interestingly, our results show that complex II is the main site of ROS production in *A. suum* adult respiratory chain (Table 1). In *A. suum* adult respiratory chain, complex II produces equally high amount of superoxide and hydrogen peroxide during the oxidation of the complex I linked substrate NADH and the complex II linked substrate succinate, even under uninhibited conditions (Table 1). This observation is contradictory to the observations so far reported for the mitochondrial respiratory chain in other organisms. Generally, the respiratory chain of isolated mammalian and avian mitochondria and submitochondrial particles respiring under uninhibited conditions produce significant amount of ROS only during succinate oxidation by complex II, but the site of ROS production is not intrinsic to complex II. In this situation, ROS are produced from complex I during the reversed flow of electrons derived from succinate oxidation to reduce NAD (Liu et al., 2002). It is completely abolished by rotenone which inhibits the Q site of complex I (Liu et al., 2002; Muller et al., 2008). One can argue that electrons originating from succinate oxidation in the mitochondrial complex II of *A. suum* adult worm also may flow in the reverse direction through the complex I and leak to oxygen, due to the absence of complexes III and IV activities in its respiratory chain. However, reversed flow of electrons through complex I was not found to be a significant mode of ROS production in the *A. suum* adult respiratory chain since inhibition of the Q site in complex I with quinazoline inhibited only 10% of the succinate-dependent ROS production (Table 1). Another feature of the *A. suum* adult respiratory chain is that it produces significantly high amount of ROS even when the succinate concentration is as low as 10 μM (Fig 3). At such lower concentrations of succinate, detectable level of ROS production is not so far reported from the mitochondrial respiratory chain in other organisms. Similar to our findings, succinate-dependent ROS production intrinsic to complex II was reported from the mitochondrial respiratory chain in *S. cerevisiae* (Guo and Lemire, 2003; Szeto et al., 2007) and *C. elegans* (Senoo-Matsuda et al., 2001; Huang and Lemire, 2009), but the amounts of ROS produced by their complex II were significantly lower than that from *A. suum* adult complex II reported in this study.

It is well established that ROS production is negligible during the oxidation of NADH linked substrates by the uninhibited mitochondrial respiratory chain, but inhibition of the Q site of complex I with an inhibitor such as rotenone results in NADH-dependent ROS production from complex I to a significant level (Hirst et al., 2008). In contrast, addition of the complex I inhibitor quinazoline or the complex II Q site inhibitor aptenin A5 during NADH oxidation in *A. suum* adult SMP almost completely abolished the ROS production detected under uninhibited conditions (Table 1), indicating that complex II is the principal ROS producing site even during NADH oxidation. Thus, our present study shows that *A. suum* adult complex II has the unique feature of significantly high amounts of intrinsic ROS production during oxidation of both the complex I and II linked substrates under uninhibited conditions.

Although it is widely accepted that complex II of the mitochondrial respiratory chain does not have an intrinsic ROS generation under physiological conditions, accumulating evidence indicates that pathogenic mutations in complex II can result in electron leak to oxygen and produce ROS. Simulation of these pathogenic mutations by pharmacological inhibition of complex II activity with thionyl trifluoroacetate (TTFA) (Eto et al., 1992; Guzy et al., 2008) and by genetic inhibition of complex II activity by RNA interference of the Ip subunit (Guzy et al., 2008) has been reported to induce succinate-dependant ROS production, probably due to formation of a flavin radical in the Fp subunit of complex II. In addition, purified and solubilized mitochondrial complex II is also shown to produce ROS through a similar manner (Zhang et al., 1998). Moreover, it has been postulated that ROS may be produced from complex II, if the enzyme is damaged by oxidative stress or ageing also (Jezek and Hlavata, 2005).

Understanding the ROS producing sites in complex II is important in addressing complex II associated diseases linked with ROS production. Currently, there are two models regarding the ROS production site in respiratory chain complex II. One model is based on studies carried out on *E. coli* complex IIs and postulates that the FAD site in the Fp subunit is the principal site of ROS production (Messner and Imlay, 2002; Yankovskaya et al., 2003). Exposure of FAD to the aqueous environment and high electron density are identified as the causes for ROS production from FAD site. This condition is a consequence of interference in electron flow through other redox centers. The other model, based on studies carried out in *S. cerevisiae*, postulates that the ubiquinone-binding site is the major ROS production site. Mutations in Ip, CybL, and CybS subunits are suggested to alter the ubiquinone-binding site, resulting in electron leak (Guo and Lemire, 2003; Szeto et al., 2007).

To gain further insight into ROS production from complex II, we used complex II of the *A. suum* adult worm since it has a high sequence similarity to mitochondrial SQR and produces a significantly high amount of ROS (Fig. 1a). As shown in Table 1, when succinate is utilized as the respiratory substrate, complete inhibition of the Q site of *A. suum* adult respiratory chain with atpenin A5 diminished the level of ROS production by 38%. Since complexes III and IV activities are not detected in *A. suum* adult respiratory chain and the contribution of complex I for succinate-dependent ROS production is not significant (Table 1), this result indicates the possibility of the Q site of the complex II in succinate-dependent ROS generation. The remaining fraction (62%) of the succinate-dependent ROS are likely to be originated from the redox centers located between the Q binding site and the succinate oxidation site in complex II. Those are the Fe-S clusters in the Ip subunit and the FAD site in the Fp subunit. Since Fe-S clusters are buried below the solvent accessible surface of the protein molecule while FAD is localized exposed to the aqueous environment (Sun et al., 2005; Yankovskaya et al., 2003), the probable contributor for the remaining fraction of the ROS appears to be the FAD site. As we have discussed in Section 3.3, the strong suppression of succinate-dependent ROS production at high concentrations of succinate provide evidence for the involvement of FAD site in succinate-dependent ROS production in *A. suum* mitochondrial

complex II. Thus, our data are in accordance with both models of ROS production from complex II (Fig. 2b).

4.1. ROS production from the FAD site

The only other complex II that is so far reported to produce such a high level of ROS from the FAD site is *E. coli* QFR. However, the Fp subunit of *A. suum* adult complex II (QFR) displayed only 37% sequence identity to that of *E. coli* QFR whereas its sequence identity to that of human Fp is much higher (68%). Moreover, the amino acid residues participating in the FAD and dicarboxylate-binding sites in *A. suum* adult complex II are identical to those in the mitochondrial SQR, but not to those in *E. coli* QFR. These observations indicate that the roles of the amino acid residues involved in interacting with FAD and substrate binding in QFR of *E. coli* and *A. suum* are different, although they share in common a high level of FRD activity and ROS production. In contrast, the SQR of *E. coli* has a low level of ROS production (Messner and Imlay, 2002). We also observed a low level of ROS production from complex II in *A. suum* L_3 larvae (Fig. 1b), which has low FRD/SQR activity (0.39) (Amino et al., 2003) despite its high sequence similarity to that of its adult counterpart.

As shown for *E. coli* complex IIs, the principal difference between SQR and QFR lies in the arrangement of redox potentials among the redox centers (Yankovskaya et al., 2003). In *E. coli* QFR, FAD and the 2Fe–2S cluster have the highest redox potentials, thus attracting electrons to fumarate. On the other hand, in *E. coli* SQR, heme *b* and 3Fe–4S have the highest redox potentials, attracting electrons to quinone. These redox potentials are known to be important to drive the electrons in the direction of the physiological reaction of the respective enzymes. Succinate oxidation in SQR and quinol oxidation in QFR leads the enzymes to a reduced state with two electrons. According to theoretical calculations, the distribution of electrons around FAD in the reduced enzyme is 50 times greater in QFR compared to that in SQR in *E. coli* (Yankovskaya et al., 2003). This provides further evidence to the proposal by Messner and Imlay (2002) that the reduced state around FAD is the cause of the high level of ROS production by *E. coli* QFR. Since complex II of *A. suum* adult worms also shows high fumarate reductase activity, it is reasonable to speculate that electrons will sequestrate on its FAD during succinate oxidation with subsequent leak to oxygen.

It appears that, despite the remarkable identity in the amino acid residues interacting with FAD and forming the substrate binding site of *A. suum* adult complex II and mitochondrial SQR, sequestration of electrons on FAD and subsequent leak to oxygen are the features mainly connected to the ability to reduce fumarate by *A. suum* adult complex II. Based on these observations, it is likely that some mutations in mitochondrial SQR may result in accumulation of electrons on FAD and subsequent leakage to oxygen. In fact, it has been shown that mitochondrial complex II produces ROS in pulmonary vasculature due to the reverse flow of electrons under hypoxic conditions (Paddenberg et al., 2003).

4.2. ROS production from the quinone binding site

As shown in Tables 1 and 2, succinate-dependent ROS production from *A. suum* SMP is considerably diminished when the complex II Q site is inhibited with atpenin A5, indicating that the quinone binding site also is a contributor for ROS production from *A. suum* complex II. The quinone binding site is formed by amino acid residues which reside in Ip, CybL, and CybS subunits. Generally, it leaks electrons to oxygen either via a destabilized quinone molecule or directly from the site. To reduce the quinone in complex II completely, two electrons are needed. However, electrons are transferred one at a time from the 3Fe–4S center to the quinone bound at the Q site. Thus, a semiquinone intermediate is an obligatory part of the quinone reduction by complex II. Until another electron arrives, the protein environment of the Q-site donates a proton and stabilizes the semiquinone, thereby preventing its release from the Q site or premature reoxidation. In the latter case, a reduction in the affinity of the Q site for quinone can result in direct transfer of electrons to oxygen from the Q site (Horsefield et al., 2006; Szeto et al., 2007).

As shown by Lemire and colleagues, using the SQR of *S. cerevisiae*, mutations in the amino acid residues associated with quinone binding and reduction lead to high levels of ROS production from the Q site (Guo and Lemire, 2003; Szeto et al., 2007). Yet, except for replacement of Ile C28 with Gly, the amino acid residues important for quinone binding and reduction in SQR enzymes are conserved in *A. suum* adult complex II. Thus, the replacement of Ile C28 to Gly seems to be responsible for ROS production, but this idea is not supported by the sequence of free-living nematode *C. elegans*, which also has Gly in that position without producing significant amounts of ROS. In addition, complex II in *S. cerevisiae*, which has Ser instead of Ile in the corresponding position, also is reported to produce very low amounts of ROS (Guo and Lemire, 2003).

When the conservation of amino acid residues responsible for quinone binding and reduction between mitochondrial SQR and *A. suum* adult complex II, which functions as QFR, are considered together with the high level of ROS production observed only from *A. suum* adult complex II, it appears that differences in the architecture of the quinone binding site caused by subtle differences in its amino acid residues may contribute to the high level of ROS production from its Q site. These differences may result in either an increase in the flow of electrons out of the enzyme or the formation of a destabilized semiquinone radical during quinone reduction, leading to a high degree of ROS production. However, we cannot rule out the possibility of the contribution of rhodoquinone for ROS production from its Q site. Rhodoquinone, which has a lower redox potential (−63 mV) compared to ubiquinone (+110 mV), is a more favorable electron donor to oxygen than ubiquinone (Kita and Takamiya, 2002). In this regard, it is also noteworthy that the Q site in *E. coli* QFR is not known to produce ROS (Messner and Imlay, 2002) despite the presence of menaquinone, which has an even lower redox potential than that of rhodoquinone (−80 mV) (Cecchini et al., 2002). Thus, the presence of a low potential quinone does not appear to be a likely cause of the high level of ROS production from the Q site in *A. suum* adult complex II.

5. Conclusion

We have shown here that under aerobic conditions, both the FAD site and quinone binding site in *A. suum* adult complex II contribute to produce significantly high amounts of O_2^- and H_2O_2 during succinate oxidation, despite its high sequence similarity to mammalian SQR, which does not produce ROS. According to our observations, subtle amino acid differences in complex II subunits may result in leakage of electrons originating from succinate oxidation from more than one site in complex II, forming ROS. Since the amino acids interacting with FAD and participating in succinate binding and quinone reduction in *A. suum* complex II are well conserved, amino acid residues responsible for high reactivity with oxygen may be localized in unique sequences in the parasite's enzyme complex.

In summary, this study shows significant release of ROS from the mitochondrial complex II using the unique *A. suum* model. We believe that *A. suum* adult complex II is a good model to study the mechanism of ROS production from mitochondrial complex II, since amino acid residues conserved among the catalytic domains

in mitochondrial SQR enzymes are well conserved in this enzyme and it produces high levels of ROS. Absence of complex III and IV activities in its respiratory chain is an additional advantage of this model. Analysis of its crystal structure and expression of its subunits in a cell-free system for mutational analysis are in progress. These studies will provide further insight into the possibility of high levels of ROS production from both the FAD site and the Q site in the complex II of *A. suum* adult worm and help to understand the role of mutations in human complex II for carcinogenesis.

Acknowledgements

This work was supported by a grant-in-aid for scientific research on Priority Areas (18073004), Creative Scientific Research (18GS0314), and Targeted Proteins Research Program to KK and by a Japanese Government scholarship to MPP from the Japanese Ministry of Education, Science, Culture, Sports and Technology.

References

Ackrell, B.A., 2002. Cytopathies involving mitochondrial complex II. Mol. Aspects. Med. 23, 369–384.

Amino, H., Osanai, A., Miyadera, H., Shinjyo, N., Tomitsuka, E., Taka, H., Mineki, R., Murayama, K., Takamiya, S., Aoki, T., Miyoshi, H., Sakamoto, K., Kojima, S., Kita, K., 2003. Isolation and characterization of the stage-specific cytochrome b small subunit (CybS) of *Ascaris suum* complex II from the aerobic respiratory chain of larval mitochondria. Mol. Biochem. Parasitol. 128, 175–186.

Amino, H., Wang, H., Hirawake, H., Saruta, F., Mizuchi, D., Mineki, R., Shindo, N., Murayama, K., Takamiya, S., Aoki, T., Kojima, S., Kita, K., 2000. Stage-specific isoforms of *Ascaris suum* complex. II: The fumarate reductase of the parasitic adult and the succinate dehydrogenase of free-living larvae share a common iron–sulfur subunit. Mol. Biochem. Parasitol. 106, 63–76.

Astuti, D., Latif, F., Dallol, A., Dahia, P.L., Douglas, F., George, E., Skoldberg, F., Husebye, E.S., Eng, C., Maher, E.R., 2001. Gene mutations in the succinate dehydrogenase subunit SDHB cause susceptibility to familial pheochromocytoma and to familial paraganglioma. Am. J. Hum. Genet. 69, 49–54.

Azzi, A., Montecucco, C., Richter, C., 1975. The use of acetylated ferricytochrome c for the detection of superoxide radicals produced in biological membranes. Biochem. Biophys. Res. Commun. 65, 597–603.

Bayley, J.P., van Minderhout, I., Weiss, M.M., Jansen, J.C., Oomen, P.H., Menko, F.H., Pasini, B., Ferrando, B., Wong, N., Alpert, L.C., Williams, R., Blair, E., Devilee, P., Taschner, P.E., 2006. Mutation analysis of SDHB and SDHC: novel germline mutations in sporadic head and neck paraganglioma and familial paraganglioma and/or pheochromocytoma. BMC Med. Genet. doi:10-1186/1471-2350-7-1.

Baysal, B.E., Ferrell, R.E., Willett-Brozick, J.E., Lawrence, E.C., Myssiorek, D., Bosch, A., van der Mey, A., Taschner, P.E., Rubinstein, W.S., Myers, E.N., Richard 3rd, C.W., Cornelisse, C.J., Devilee, P., Devlin, B., 2000. Mutations in SDHD, a mitochondrial complex II gene, in hereditary paraganglioma. Science 287, 848–851.

Baysal, B.E., Willett-Brozick, J.E., Lawrence, E.C., Drovdlic, C.M., Savul, S.A., McLeod, D.R., Yee, H.A., Brackmann, D.E., Slattery 3rd, W.H., Myers, E.N., Ferrell, R.E., Rubinstein, W.S., 2002. Prevalence of SDHB, SDHC, and SDHD germline mutations in clinic patients with head and neck paragangliomas. J. Med. Genet. 39, 178–183.

Bourgeron, T., Rustin, P., Chretien, D., Birch-Machin, M., Bourgeois, M., Viegas-Pequignot, E., Munnich, A., Rotig, A., 1995. Mutation of a nuclear succinate dehydrogenase gene results in mitochondrial respiratory chain deficiency. Nat. Genet. 11, 144–149.

Briere, J.J., Favier, J., Benit, P., El Ghouzzi, V., Lorenzato, A., Rabier, D., Di Renzo, M.F., Gimenez-Roqueplo, A.P., Rustin, P., 2005. Mitochondrial succinate is instrumental for HIF1alpha nuclear translocation in SDHA-mutant fibroblasts under normoxic conditions. Hum. Mol. Genet. 14, 3263–3269.

Cecchini, G., Schroder, I., Gunsalus, R.P., Maklashina, E., 2002. Succinate dehydrogenase and fumarate reductase from *Escherichia coli*. Biochim. Biophys. Acta. 1553, 140–157.

Cervera, A.M., Apostolova, N., Crespo, F.L., Mata, M., McCreath, K.J., 2008. Cells silenced for SDHB expression display characteristic features of the tumor phenotype. Cancer Res. 68, 4058–4067.

Chen, Q., Vazquez, E.J., Moghaddas, S., Hoppel, C.L., Lesnefsky, E.J., 2003. Production of reactive oxygen species by mitochondria: central role of complex III. J. Biol. Chem. 278, 36027–36031.

Eng, C., Kiuru, M., Fernandez, M.J., Aaltonen, L.A., 2003. A role for mitochondrial enzymes in inherited neoplasia and beyond. Nat. Rev. Cancer 3, 193–202.

Eto, Y., Kang, D., Hasegawa, E., Takeshige, K., Minakami, S., 1992. Succinate-dependent lipid peroxidation and its prevention by reduced ubiquinone in beef heart submitochondrial particles. Arch. Biochem. Biophys. 295, 101–106.

Guo, J., Lemire, B.D., 2003. The ubiquinone-binding site of the *Saccharomyces cerevisiae* succinate–ubiquinone oxidoreductase is a source of superoxide. J. Biol. Chem. 278, 47629–47635.

Guzy, R.D., Sharma, B., Bell, E., Chandel, N.S., Schumacker, P.T., 2008. Loss of the SdhB, but Not the SdhA, subunit of complex II triggers reactive oxygen species-dependent hypoxia-inducible factor activation and tumorigenesis. Mol. Cell Biol. 28, 718–731.

Hirst, J., King, M.S., Pryde, K.R., 2008. The production of reactive oxygen species by complex I. Biochem. Soc. Trans. 36, 976–980.

Horsefield, R., Yankovskaya, V., Sexton, G., Whittingham, W., Shiomi, K., Omura, S., Byrne, B., Cecchini, G., Iwata, S., 2006. Structural and computational analysis of the quinone-binding site of complex II (succinate–ubiquinone oxidoreductase): a mechanism of electron transfer and proton conduction during ubiquinone reduction. J. Biol. Chem. 281, 7309–7316.

Huang, J., Lemire, B.D., 2009. Mutations in the *C. elegans* succinate dehydrogenase iron-sulfur subunit promote superoxide generation and premature aging. J. Mol. Biol. 387, 559–569.

Huang, L.S., Shen, J.T., Wang, A.C., Berry, E.A., 2006. Crystallographic studies of the binding of ligands to the dicarboxylate site of Complex II, and the identity of the ligand in the "oxaloacetate-inhibited" state. Biochim. Biophys. Acta 1757, 1073–1083.

Imlay, J.A., Fridovich, I., 1991. Assay of metabolic superoxide production in *Escherichia coli*. J. Biol. Chem. 266, 6957–6965.

Indo, H.P., Davidson, M., Yen, H.C., Suenaga, S., Tomita, K., Nishii, T., Higuchi, M., Koga, Y., Ozawa, T., Majima, H.J., 2007. Evidence of ROS generation by mitochondria in cells with impaired electron transport chain and mitochondrial DNA damage. Mitochondrion 7, 106–118.

Ishii, T., Sakurai, T., Usami, H., Uchida, K., 2005. Oxidative modification of proteasome: identification of an oxidation-sensitive subunit in 26S proteasome. Biochemistry 44, 13893–13901.

Iwata, F., Shinjyo, N., Amino, H., Sakamoto, K., Islam, M.K., Tsuji, N., Kita, K., 2008. Change of subunit composition of mitochondrial complex II (succinate–ubiquinone reductase/quinol-fumarate reductase) in *Ascaris suum* during the migration in the experimental host. Parasitol. Int. 57, 54–61.

Jezek, P., Hlavata, L., 2005. Mitochondria in homeostasis of reactive oxygen species in cell, tissues, and organism. Int. J. Biochem. Cell Biol. 37, 2478–2503.

Kita, K., Hirawake, H., Miyadera, H., Amino, H., Takeo, S., 2002. Role of complex II in anaerobic respiration of the parasite mitochondria from *Ascaris suum* and *Plasmodium falciparum*. Biochim. Biophys. Acta 1553, 123–139.

Kita, K., Takamiya, S., 2002. Electron-transfer complexes in Ascaris mitochondria. Adv. Parasitol. 51, 95–131.

Kita, K., Shiomi, K., Ōmura, S., 2007. Parasitology in Japan: advances in drug discovery and biochemical studies. Trends. Parasitol. 23, 223–229.

Kuramochi, T., Hirawake, H., Kojima, S., Takamiya, S., Furushima, R., Aoki, T., Komuniecki, R., Kita, K., 1994. Sequence comparison between the flavoprotein subunit of the fumarate reductase (complex II) of the anaerobic parasitic nematode, *Ascaris suum* and the succinate dehydrogenase of the aerobic, free-living nematode, *Caenorhabditis elegans*. Mol. Biochem. Parasitol. 68, 177–187.

Lancaster, C.R.D., 2004. Structure and function of succinate: quinone oxidoreductases and the role of quinol: fumarate reductases in fumarate respiration. In: Zannoni, D. (Ed.), Respiration in Archaea and Bacteria: Diversity of Prokaryotic Electron Transport Carriers. Kluwer Academic Publishers, The Netherlands, pp. 57–85.

Liu, Y., Fiskum, G., Schubert, D., 2002. Generation of reactive oxygen species by the mitochondrial electron transport chain. J. Neurochem. 80, 780–787.

Lowry, O.H., Rosebrough, N.J., Farr, A.L., Randall, R.J., 1951. Protein measurement with the Folin phenol reagent. J. Biol. Chem. 193, 265–275.

Matsumoto, J., Sakamoto, K., Shinjyo, N., Kido, Y., Yamamoto, N., Yagi, K., Miyoshi, H., Nonaka, N., Katakura, K., Kita, K., Oku, Y., 2008. Anaerobic NADH-fumarate reductase system is predominant in the respiratory chain of *Echinococcus multilocularis*, providing a novel target for the chemotherapy of alveolar echinococcosis. Antimicrob. Agents Chemother. 52, 164–170.

Matsuno-Yagi, A., Hatefi, Y., 1985. Studies on the mechanism of oxidative phosphorylation. Catalytic site cooperativity in ATP synthesis. J. Biol. Chem. 260, 11424–11427.

Messner, K.R., Imlay, J.A., 2002. Mechanism of superoxide and hydrogen peroxide formation by fumarate reductase, succinate dehydrogenase, and aspartate oxidase. J. Biol. Chem. 277, 42563–42571.

Miyadera, H., Shiomi, K., Ui, H., Yamaguchi, Y., Masuma, R., Tomoda, H., Miyoshi, H., Osanai, A., Kita, K., Omura, S., 2003. Atpenins, potent and specific inhibitors of mitochondrial complex II (succinate–ubiquinone oxidoreductase). Proc. Natl. Acad. Sci. USA 100, 473–477.

Mohanty, J.G., Jaffe, J.S., Schulman, E.S., Raible, D.G., 1997. A highly sensitive fluorescent micro-assay of H2O2 release from activated human leukocytes using a dihydroxyphenoxazine derivative. J. Immunol. Methods 202, 133–141.

Muller, F.L., Liu, Y., Abdul-Ghani, M.A., Lustgarten, M.S., Bhattacharya, A., Jang, Y.C., Van Remmen, H., 2008. High rates of superoxide production in skeletal-muscle mitochondria respiring on both complex I- and complex II-linked substrates. Biochem. J. 409, 491–499.

Murphy, M.P., 2009. How mitochondria produce reactive oxygen species. Biochem. J. 417, 1–13.

Ni, Y., Zbuk, K.M., Sadler, T., Patocs, A., Lobo, G., Edelman, E., Platzer, P., Orloff, M.S., Waite, K.A., Eng, C., 2008. Germline mutations and variants in the succinate dehydrogenase genes in Cowden and Cowden-like syndromes. Am. J. Hum. Genet. 83, 261–268.

Paddenberg, R., Ishaq, B., Goldenberg, A., Faulhammer, P., Rose, F., Weissmann, N., Braun-Dullaeus, R.C., Kummer, W., 2003. Essential role of complex II of the respiratory chain in hypoxia-induced ROS generation in the pulmonary vasculature. Am. J. Physiol. Lung. Cell. Mol. Physiol. 284, L710–719.

Saruta, F., Hirawake, H., Takamiya, S., Ma, Y.C., Aoki, T., Sekimizu, K., Kojima, S., Kita, K., 1996. Cloning of a cDNA encoding the small subunit of cytochrome b558 (cybS) of mitochondrial fumarate reductase (complex II) from adult *Ascaris suum*. Biochim. Biophys. Acta. 1276, 1–5.

Saruta, F., Kuramochi, T., Nakamura, K., Takamiya, S., Yu, Y., Aoki, T., Sekimizu, K., Kojima, S., Kita, K., 1995. Stage-specific isoforms of complex II (succinate–ubiquinone oxidoreductase) in mitochondria from the parasitic nematode, *Ascaris suum*. J. Biol. Chem. 270, 928–932.

Senoo-Matsuda, N., Yasuda, K., Tsuda, M., Ohkubo, T., Yoshimura, S., Nakazawa, H., Hartman, P.S., Ishii, N., 2001. A defect in the cytochrome b large subunit in complex II causes both superoxide anion overproduction and abnormal energy metabolism in *Caenorhabditis elegans*. J. Biol. Chem. 276, 41553–41558.

Selak, M.A., Armour, S.M., MacKenzie, E.D., Boulahbel, H., Watson, D.G., Mansfield, K.D., Pan, Y., Simon, M.C., Thompson, C.B., Gottlieb, E., 2005. Succinate links TCA cycle dysfunction to oncogenesis by inhibiting HIF-alpha prolyl hydroxylase. Cancer Cell 7, 77–85.

Shinjyo, N., Kita, K., 2007. Relationship between reactive oxygen species and heme metabolism during the differentiation of Neuro2a cells. Biochem. Biophys. Res. Commun. 358, 130–135.

St-Pierre, J., Buckingham, J.A., Roebuck, S.J., Brand, M.D., 2002. Topology of superoxide production from different sites in the mitochondrial electron transport chain. J. Biol. Chem. 277, 44784–44790.

Sun, F., Huo, X., Zhai, Y., Wang, A., Xu, J., Su, D., Bartlam, M., Rao, Z., 2005. Crystal structure of mitochondrial respiratory membrane protein complex II. Cell 121, 1043–1057.

Szeto, S.S., Reinke, S.N., Sykes, B.D., Lemire, B.D., 2007. Ubiquinone-binding site mutations in the *Saccharomyces cerevisiae* succinate dehydrogenase generate superoxide and lead to the accumulation of succinate. J. Biol. Chem. 282, 27518–27526.

Takamiya, S., Furushima, R., Oya, H., 1986. Electron transfer complexes of Ascaris suum muscle mitochondria. II. Succinate–coenzyme Q reductase (complex II) associated with substrate-reducible cytochrome *b*558. Biochim. Biophys. Acta 848, 99–107.

Van Hellmond, J.J., van der Klei, A., van Weelden, S.W.H., Tielens, A.G.M., 2003. Biochemical and evolutionary aspects of anaerobically functioning bacteria. Phil. Trans. R. Soc. B. 358, 205–215.

Yamashita, T., Ino, T., Miyoshi, H., Sakamoto, K., Osanai, A., Nakamaru-Ogiso, E., Kita, K., 2004. Rhodoquinone reaction site of mitochondrial complex I, in parasitic helminth, *Ascaris suum*. Biochim. Biophys. Acta 1608, 97–103.

Yankovskaya, V., Horsefield, R., Tornroth, S., Luna-Chavez, C., Miyoshi, H., Leger, C., Byrne, B., Cecchini, G., Iwata, S., 2003. Architecture of succinate dehydrogenase and reactive oxygen species generation. Science 299, 700–704.

Zhang, L., Yu, L., Yu, C.A., 1998. Generation of superoxide anion by succinate–cytochrome c reductase from bovine heart mitochondria. J. Biol. Chem. 273, 33972–33976.

Zhao, Z., Rothery, R.A., Weiner, J.H., 2006. Effects of site-directed mutations in *Escherichia coli* succinate dehydrogenase on the enzyme activity and production of superoxide radicals. Biochem. Cell Biol. 84, 1013–1021.

ELSEVIER

Journal of Hepatology 51 (2009) 333–341

Journal of Hepatology

www.elsevier.com/locate/jhep

Contribution of TIR domain-containing adapter inducing IFN-β-mediated IL-18 release to LPS-induced liver injury in mice☆

Michiko Imamura[1,2,3], Hiroko Tsutsui[2,*], Koubun Yasuda[3], Ryosuke Uchiyama[2], Shizue Yumikura-Futatsugi[3], Keiko Mitani[1], Shuhei Hayashi[2], Shizuo Akira[4], Shun-ichiro Taniguchi[5], Nico Van Rooijen[6], Jurg Tschopp[7], Tetsuya Yamamoto[8], Jiro Fujimoto[1], Kenji Nakanishi[3,9,*]

[1]*Department of Surgery, Hyogo College of Medicine, Nishinomiya, Japan*
[2]*Department of Microbiology, Hyogo College of Medicine, 1-1, Mukogawa-cho, Hyogo 663-8501, Nishinomiya, Japan*
[3]*Department of Immunology & Medical Zoology, Hyogo College of Medicine, Nishinomiya, Japan*
[4]*Department of Innate Immunity, Research Institutes for Microbiological Diseases, Osaka University, Suita, Japan*
[5]*Department of Molecular Oncology, Institute on Aging and Adaptation, Shinshu University, Graduate School of Medicine, Matsumoto, Japan*
[6]*Department of Cell Biology and Immunology, Free University, Amsterdam, The Netherlands*
[7]*Department of Biochemistry, University of Lausanne, Switzerland*
[8]*Department of Internal Medicine, Hyogo College of Medicine, Nishinomiya, Japan*
[9]*Collaborative Development of Innovation Seeds, Japan Science and Technology Agency, Tokyo, Japan*

***Background/Aims*: After treatment with heat-killed *Propionibacterium acnes* mice show dense hepatic granuloma formation. Such mice develop liver injury in an interleukin (IL)-18-dependent manner after challenge with a sublethal dose LPS. As previously shown, LPS-stimulated Kupffer cells secrete IL-18 depending on caspase-1 and Toll-like receptor (TLR)-4 but independently of its signal adaptor myeloid differentiation factor 88 (MyD88), suggesting importance of another signal adaptor TIR domain-containing adapter inducing IFN-β (TRIF). Nalp3 inflammasome reportedly controls caspase-1 activation. Here we investigated the roles of MyD88 and TRIF in *P. acnes*-induced hepatic granuloma formation and LPS-induced caspase-1 activation for IL-18 release.**

***Methods*: Mice were sequentially treated with *P. acnes* and LPS, and their serum IL-18 levels and liver injuries were determined by ELISA and ALT/AST measurement, respectively. Active caspase-1 in LPS-stimulated Kupffer cells was determined by Western blotting.**

***Results*: Macrophage-ablated mice lacked *P. acnes*-induced hepatic granuloma formation and LPS-induced serum IL-18 elevation and liver injury. *Myd88*$^{-/-}$ Kupffer cells, but not *Trif*$^{-/-}$ cells, exhibited normal caspase-1 activation upon TLR4 engagement *in vitro*. *Myd88*$^{-/-}$ mice failed to develop hepatic granulomas after *P. acnes* treatment and liver injury induced by LPS challenge. In contrast, *Trif*$^{-/-}$ mice normally formed the hepatic granulomas, but could not release IL-18 or develop the liver injury. *Nalp3*$^{-/-}$ mice showed the same phenotypes of *Trif*$^{-/-}$ mice.**

***Conclusions*: *Propionibacterium acnes* treatment MyD88-dependently induced hepatic granuloma formation. Subsequent LPS TRIF-dependently activated caspase-1 via Nalp3 inflammasome and induced IL-18 release, eventually leading to the liver injury.**

Keywords: Liver injury; LPS; IL-18; TRIF; Nalp3 inflammasome

Received 6 January 2009; received in revised form 28 February 2009; accepted 12 March 2009; available online 20 May 2009
Associate Editor: C. Trautwein

☆ The authors who have taken part in this study declared that they do not have anything to disclose regarding funding from industry or conflict of interest with respect to this manuscript.

* Corresponding authors. Tel.: +81 798 456547/+81 798 456572; fax: +81 798 409162/+81 798 405423.
E-mail addresses: gorichan@hyo-med.ac.jp (H. Tsutsui), nakaken@hyo-med.ac.jp (K. Nakanishi).

Abbreviations: Ab, antibody; ASC, Apoptosis-associated speck-like protein containing a caspase recruitment domain; IL, interleukin; mAb, monoclonal antibody; MyD88, myeloid differentiation factor 88; Pro, precursor; TLR, Toll-like receptor; TRIF, TIR domain-containing adapter inducing IFN-β; WT, wild-type.

0168-8278/$36.00
doi:10.1016/j.jhep.2009.03.027

1. Introduction

Toll-like receptor (TLR) signaling that is independently controlled by myeloid differentiation factor 88 (MyD88) and TIR domain-containing adapter inducing IFN-β (TRIF) [1], is important for the liver in health (host defense and liver regeneration) and disease (inflammation) [2]. Liver possesses robust innate immune cells expressing TLRs, such as Kupffer cells and NK cells [2–4]. After partial hepatectomy, Kupffer cells in the remnant liver promptly produce TNF-α in a MyD88-dependent manner, which in turn induces IL-6 production, eventually leading to homeostatic liver regeneration [5–7]. Following microbial infection, Kupffer cells produce IL-12 MyD88-dependently, which initiates IFN-γ production for microbial eradication in the early infection phase [3,4,8,9]. Thus, the TLR/MyD88-mediated signalings are beneficial in the liver homeostasis. Simultaneously, TLR-mediated signals induce severe liver inflammation. As previously reported wild-type (WT) mice primed with heat-killed *Propionibacterium acnes* develop dense hepatic granulomas. These *P. acnes*-primed mice undergo acute inflammatory liver injury whenever being subsequently challenged with a sublethal dose of LPS (<50 μg/kg [3,10]. However, as shown previously, *Il12p40*$^{-/-}$ mice and *Ifnγ*$^{-/-}$ mice lack the dense hepatic granuloma formation after *P. acnes* treatment and never exhibit liver injury after LPS challenge [11,12], suggesting importance of IL-12/IFN-γ for the sensitization to LPS induced by *P. acnes* treatment. Furthermore, *P. acnes*-primed *Myd88*$^{-/-}$ mice have poor formation of hepatic granulomas and are resistant to liver injury following LPS challenge [13], suggesting importance of MyD88-dependently produced IL-12/IFN-γ for *P. acnes*-induced sensitization to LPS. In contrast, IL-18 accounts for this liver injury by induction of hepatocytotoxic Fas ligand and TNF-α after LPS challenge [3,10,14–16]. Indeed, IL-18 blockade at LPS challenge can prevent *P. acnes*-primed mice that possess dense hepatic granulomas from this liver injury [10,17]. Furthermore, *Il18*$^{-/-}$ mice normally develop hepatic granulomas after *P. acnes* treatment, but can evade liver injury after LPS challenge [11]. Thus, it is very important to reveal the mechanism how IL-18 is released in response to LPS. We and others previously reported that IL-18, like IL-1β, is produced as biologically inactive precursor (pro) and becomes active after cleavage by caspase-1 [18–21]. Caspase-1 is also produced as inactive zymogen and needs appropriate stimuli to become active. However, it is unclear how TLR4 signaling activates caspase-1 for IL-18 release and which cell type is mainly involved in IL-18 release *in vivo*.

Accumulated lines of evidence demonstrated that Nalp3 inflammasome is important for activation of caspase-1 [22]. Here we first showed that *Trif*$^{-/-}$ mice, but not *Myd88*$^{-/-}$ mice, develop hepatic granulomas after *P. acnes* treatment but that both genotypes of mice evade the liver injury following LPS challenge. *Myd88*$^{-/-}$ Kupffer cells as well as WT Kupffer cells could secrete IL-18 in response to TLR4 agonist [8], while *Trif*$^{-/-}$cells could not, suggesting that the TLR4/TRIF-signaling activates caspase-1. Furthermore, *Nalp3*$^{-/-}$ mice, like *Trif*$^{-/-}$mice, could not increase serum IL-18 or develop liver injury after *P. acnes* pretreatment and subsequent LPS challenge. Thus, the TLR4/TRIF signaling induces liver injury by Nalp3-dependent activation of caspase-1.

As named inflammasome, this component plays a critical role in induction of inflammation through caspase-1 activation [22,23]. Production of IL-18 and IL-1β is principally dependent on caspase-1 activation, and levels of these cytokines are tightly associated with severity of inflammation [22,23]. TLR delivers signals via two distinct pathways. MyD88-dependent signal is for induction of host defense and liver regeneration. In contrast, TRIF-dependent signal induces inflammation via activating caspase-1. Therefore, it is conceivable that IL-18 released by Kupffer cells/hepatic macrophages is profoundly involved in the development of liver injury initiated by the TLR4 engagement.

2. Materials and methods

2.1. Mice

Trif$^{-/-}$ mice [24] on a C57BL/6 (B6) 129 background were back-crossed with B6 mice ten times and more. *Myd88*$^{-/-}$mice [25] and *Nalp3*$^{-/-}$ mice [26] on a B6 background were described elsewhere. *P2x7r*$^{-/-}$ B6 129 mice from Jackson Laboratory were back-crossed with B6 mice, and F3 littermates were used. B6 mice were purchased from Clea Japan (Osaka, Japan). Female mice (8–12 week-old) were used. All mice were maintained under specific pathogen-free conditions, and received humane care as outlined in the Guide for the Care and Use of Experimental Animals in Hyogo College of Medicine.

2.2. Reagents

LPS from *Escherichia coli* (O55: B5) was from Sigma (St. Luis, MO). Synthetic lipid A (Compound 506) was kindly provided by Dr. Fujimoto at Osaka University (Osaka, Japan) [8]. Heat-killed *P. acnes* was prepared [15]. Liposome-encapsulated dichloromethylene bisphosphonate (clodronate liposome) and PBS liposome were described elsewhere [27]. Caspase inhibitor z-VAD-fmk was purchased from Peptide Institute (Osaka, Japan) [15]. Preparation of monosodium urate crystal was described elsewhere [28].

2.3. Preparation of Kupffer cells

Kupffer cells (Supplementary method) (4×10^6 cells/well) were incubated in 1 ml of opti-MEM (Invitrogen, Calsbad, CA) supplemented with 0.001% fetal calf serum and 10 μg/ml of lipid A in a 6-well plate for 4.5 h. Supernatants and cells were separately collected for Western blotting analysis or ELISA [8]. In some experiments Kupffer cells in RPMI1640-based medium [8] (2×10^6 cells/well in a 24 well-plate) were incubated with monosodium urate crystal for 16 h and supernatants were harvested for measurement of cytokines by ELISA.

2.4. Western blotting analysis

Supernatants were concentrated using trichloroacetate [26]. The cell lysate sample was prepared [8]. Molecular sizes of IL-1β and caspase-1 in each preparation were determined by Western blotting [5]. The primary antibodies (Abs) used were: anti-mouse IL-1β Abs (Santa Cruise) and anti-caspase-1 p10 Abs (Santa Cruise). Densitometric analysis for active caspase-1 of independent experiments was performed [5], and calculated as follows:

Relative expression of active caspase-1 = densitometric data of active caspase-1 released from stimulated Kupffer cells/those from unstimulated cells.

2.5. Sequential treatment with P. acnes and LPS

Propionibacterium acnes-primed mice were challenged with 50 μg/kg of LPS at day 7 [8,17,29]. In some experiments, mice were administered intravenously with 200 μl of clodronate liposome at −2 and +5 days after *P. acnes* treatment. In some experiments, *P. acnes*-primed mice were additionally administered *iv* with 200 μg of z-VAD-fmk at 1 h before LPS challenge [15,30]. Sera were sampled for measurement of cytokine levels by ELISA [8] and of ALT levels (SRL, Tokyo Japan).

2.6. Immuno-histological analysis

Liver slices were incubated with a battery of anti-F4/80 mAb (BMA, Augst, Switzerland) and rhodamine-labeled anti-rat IgG [5], followed by counter-staining with hematoxylin.

2.7. Confocal microscopic analysis

Frozen sections of liver specimens were incubated with F4/80 mAb, biotinylated anti-rat IgG, and then Alexa Fluor 488-conjugated streptavidin (Molecular Probes). Nuclei were stained by DAPI (KPL, Gaitherburg, MD). The immunostaining of each section was evaluated using a laser scanning confocal microscopy [31].

2.8. Statistics

All data are shown as the mean ± SD of triplicate samples. Five to ten mice were used for each experimental group *in vivo*. Significance was examined by the unpaired Student *t* test. *p* values less than 0.05 were considered significant. Two to three experiments were performed, and representative data were shown in the figures.

3. Results

3.1. Importance of macrophages for the development of liver injury with elevated serum IL-18

Since many cell types can produce IL-18 [16], we analyzed whether macrophage is a major cell source of IL-18 in *P. acnes*-primed and LPS-challenged mice. It is well documented that intravenous administration of clodronate liposome can eliminate macrophages including Kupffer cells [27]. Consistent with our previous report [11,17], *P. acnes* treatment induced dense hepatic granulomas consisting of $F4/80^+$ macrophages (Fig. 1A, B). A single injection of clodronate liposome could not abolish hepatic granulomas (Supplementary Fig. 1). Twice injections could eliminate the hepatic granuloma formation (Fig. 1C), whereas control PBS liposome did not reduce it (Fig. 1B, described below). Notably, clodronate liposome administration inhibited increase in serum IL-18 (Fig. 1D) and protected against *P. acnes*/LPS-induced liver injury (Fig. 1F and G), while control mice exhibited both of them (Fig. 1D, E and G). These results demonstrated that macrophages predominantly contribute to the elevated serum IL-18 and to the development of liver injury.

3.2. Dispensability of TRIF for hepatic granuloma formation

Propionibacterium acnes-induced hepatic granuloma is necessary for the liver injury after LPS challenge (Fig. 1B, C, E, F and G). In fact, naïve mice did not develop liver injury or release IL-18 after LPS challenge (Supplementary Fig. 2). Thus, *P.* acnes treatment induces sensitization to LPS in WT mice possibly by induction of hepatic granuloma formation. Recent study showed involvement of MyD88 in the formation of hepatic granuloma [13]. Consistent with this, microscopic analysis revealed loss of granuloma formation in $Myd88^{-/-}$ mice (Fig. 2A and C). In contrast, $Trif^{-/-}$ mice possessed comparable hepatic granulomas (Fig. 2A and B), indicating dispensability of TRIF.

3.3. Requirement of both TRIF and MyD88 signals for the development of liver injury

Although it is dispensable for the hepatic granuloma formation (Fig. 2B), TRIF is necessary for the development of *P. acnes*/LPS-induced liver injury (Fig. 2D, E and G). Consistently $Myd88^{-/-}$ mice evaded this liver injury (Fig. 2F and G). Taken together, these results clearly demonstrated that both TRIF and MyD88 are necessary for the liver injury [11,17].

3.4. Both TRIF and MyD88 are required for in vivo release of IL-18

Next, we investigated whether both genotypes of mice lack IL-18 release relevant to the liver injury. C3H/HeJ mice genetically deficient in TLR4 signaling failed to increase serum IL-18 as compared to the congenic WT C3H/HeN mice (Supplementary Fig. 3), confirming LPS used as an accurate ligand for TLR4. Expectedly, *P. acnes*-primed $Myd88^{-/-}$ mice completely lacked the serum elevation of IL-18 after LPS challenge (Fig. 2H). $Trif^{-/-}$ mice, despite normal hepatic granuloma formation, lacked serum increase of IL-18 (Fig. 2H), suggesting that TRIF signal contribute to the liver injury by induction of release of IL-18.

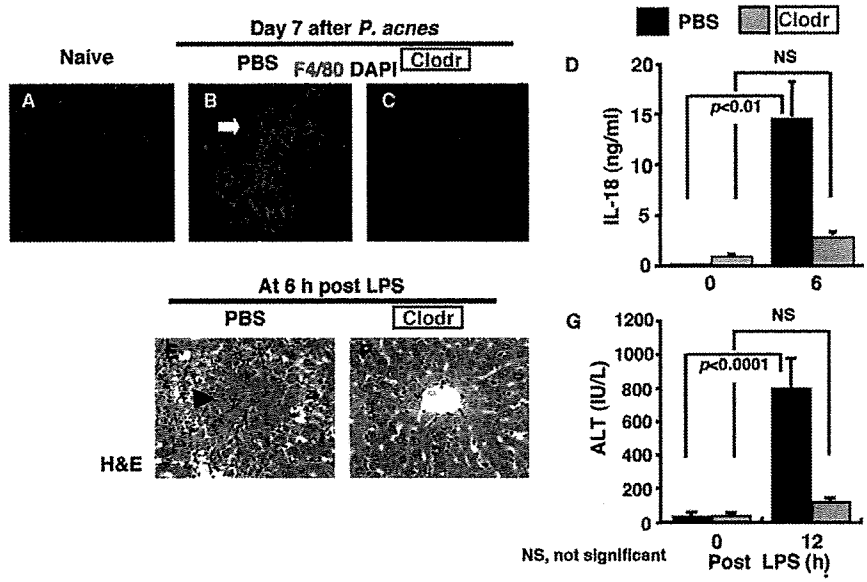

Fig. 1. Importance of macrophages for both elevated serum IL-18 and liver injury induced by sequential treatment with *P. acnes* and LPS. WT mice administered without (A) or with heat-killed *P. acnes* (B–G) were challenged without (A–C) or with LPS (D–G) at day 7. At day −2 and +5, mice were additionally administered with PBS liposome (PBS, black bars, B, D, E, and G) or clodronate liposome (Clodr, gray bars, C, D, F, and G). Liver specimens and sera were sampled for analysis of distribution of $F4/80^+$ cells (green) (A–C) and histological analysis (E and F), and measurement of IL-18 (D) and ALT (G), respectively. Original magnification; 200× (A–C), 100× (E and F). Arrow indicates hepatic granuloma, and arrowhead shows necrotic locus.

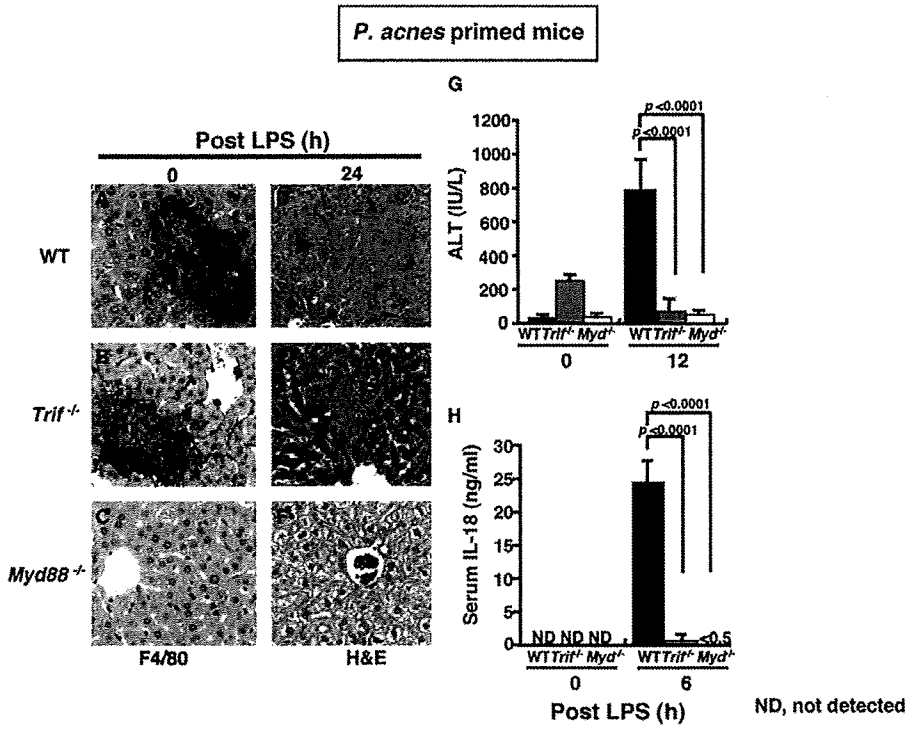

Fig. 2. Both MyD88 and TRIF are necessary for the liver injury. Liver specimens and sera were sampled from *P. acnes*-primed WT (A, D, G, and H), *Trif*$^{-/-}$(B,E, G, and H), or *Myd88*$^{-/-}$ mice (C, F, G, and H) at the indicated time points after LPS challenge for detection of macrophage localization by staining liver sections with anti-F4/80 mAb (F4/80) (A–C) and histological study (H&E) (D, E, and F), and for measurement of ALT levels (G) and IL-18 concentrations (H), respectively. Arrows indicate hepatic granulomas, and an arrowhead indicates necrotic lesion. Original magnification: 100×.

3.5. Requirement of caspase-1 for in vivo release of IL-18

Consistent with our previous report showing loss of serum IL-18 elevation in *Caspase-1*$^{-/-}$ mice after sequential treatment with *P. acnes* and LPS [20], additional administration of caspase inhibitor z-VAD at LPS challenge hampered serum increase of caspase-1-dependent IL-18 and IL-1β, but completely not caspase-1–independent IL-6, in *P. acnes*-primed WT mice (Fig. 3). These results clearly indicated that caspase-1 is activated during the effector phase after LPS challenge.

3.6. Importance of TRIF, but not MyD88, for the TLR4-mediated caspase-1 activation

We wanted to know whether TRIF is involved in the caspase-1 activation after LPS challenge. To verify this we incubated Kupffer cells with lipid A, an active component of LPS and analyzed active caspase-1 in their supernatant and cell lysate by Western blotting analyses. Lack of caspase-1 activation in lipid A-stimulated *Tlr4*$^{-/-}$ cells demonstrated this lipid A as an appropriate TLR4 agonist (Supplementary Fig. 4). Consistent with our previous report [8], *Myd88*$^{-/-}$ Kupffer cells exhibited comparable activation of caspase-1 (Fig. 4B and D). In contrast, *Trif*$^{-/-}$ Kupffer cells could not process pro-caspase-1 (Fig. 4A and C), indicating importance of TRIF for the TLR4-mediated caspase-1 activation. To prove the enzymatic capacity of active caspase-1 we analyzed IL-1β processing. Expectedly, WT Kupffer cells, but not *Tlr4*$^{-/-}$ cells, processed IL-1β after stimulation with lipid A (Supplementary Fig. 4). As they were severely impaired in pro-IL-1β production, *Myd88*$^{-/-}$ Kupffer cells could not release mature IL-1β despite their normal activation of caspase-1 (Fig. 4B, D and F). Inversely, *Trif*$^{-/-}$ Kupffer cells normally produced pro-IL-1β but failed in release of mature IL-1 β Fig. 4A, C and E), clearly indicating that their lack of IL-1β release is attributable to their impaired caspase-1 activation (Fig. 4A and C). These results clearly demonstrated importance of TRIF, but not MyD88, for the TLR4-mediated caspase-1 activation and that the absence of caspase-1 activation in *Trif*$^{-/-}$ mice results in loss of the elevated serum IL-18 and in their escape from the liver injury.

3.7. Dispensability of endogenous ATP for the development of liver injury

ATP signaling has been reported to be important for caspase-1 activation in mouse peritoneal exudate macrophages [22,23]. To exclude the possible involvement of endogenous ATP in the release of IL-18 *in vivo*, we investigated whether mice deficient in cell surface ATP receptor, $P2x_7R$, can evade the IL-18-involved liver injury [32]. *P2x7r*$^{-/-}$ mice exhibited comparable elevation of serum IL-18 as in WT littermates after sequential treatment with *P. acnes* and LPS (Fig. 5A). Furthermore, *P2x7r*$^{-/-}$ mice could form the dense hepatic granulomas (Fig. 5C) and suffered from the liver injury (Fig. 5E and F) comparably as did *P2x7r*$^{+/-}$ mice (Fig. 5B, D and F). *In vitro* study also revealed that *P2x7*$^{-/-}$ Kupffer cells exhibit normal caspase-1 activation and release comparable IL-18 and IL-1β (Supplementary Fig. 5), verifying dispensability of endogenous ATP signaling. Thus, ATP signaling is not involved in the IL-18 production or the liver injury.

3.8. Importance of Nalp3 inflammasome

Nalp3 inflammasome is composed of cytoplasmic sensor, Nalp3 protein, and caspase-1 activation adaptor, Apoptosis-associated speck-like protein containing a caspase recruitment domain (ASC). Nalp3 inflammasome controls caspase-1 activation in various situations [22]. Furthermore, as previously reported, Asc$^{-/-}$ mice lacked the elevation of serum IL-18 and evaded the liver injury [29]. Therefore, we wanted to know a role for Nalp3 protein. The elevated serum IL-18 was absent in Nalp3$^{-/-}$ mice (Fig. 6A) despite normal hepatic granuloma formation after *P. acnes* treatment (Fig. 6B and

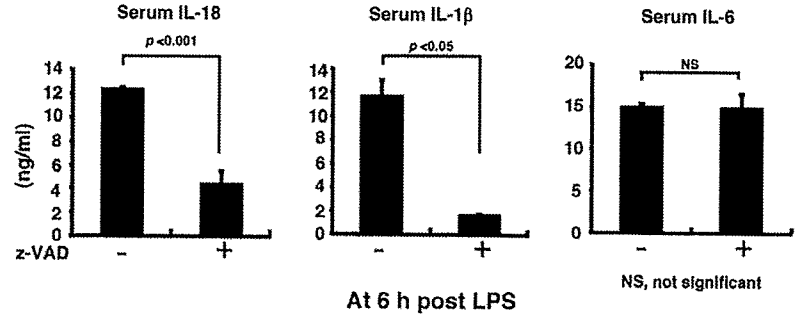

Fig. 3. Impaired serum increase of IL-1β and IL-18 but not IL-6 by treatment with caspase inhibitor. *P. acnes*-primed WT mice were administered with z-VAD 1 h before LPS challenge. At 6 h after LPS challenge sera were sampled for measurement of IL-18, IL-1β, and IL-6.

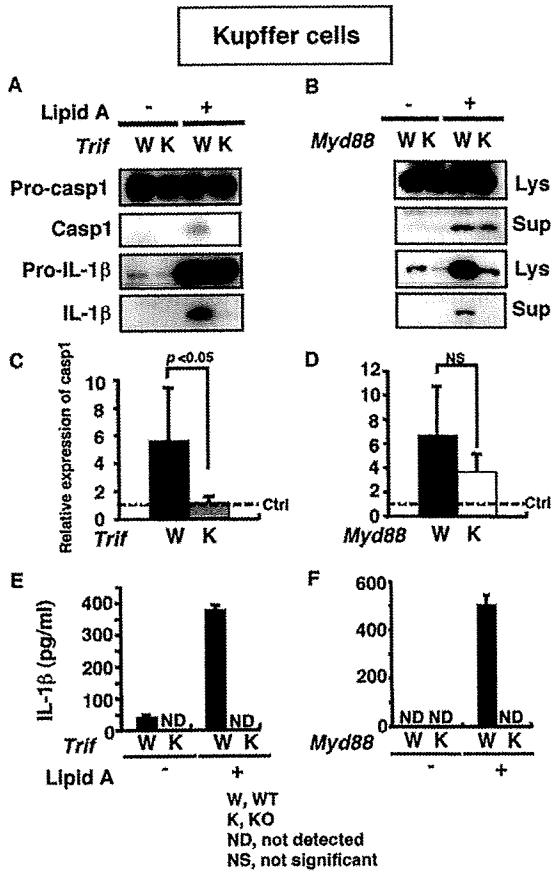

Fig. 4. TRIF but not MyD88 is essential for the lipid A-induced caspase-1 activation in Kupffer cells. Kupffer cells from WT mice (W) (A–F), *Trif*$^{-/-}$mice (K) (A, C, and E), or *Myd88*$^{-/-}$ mice (K) (B, D and F) were incubated with lipid A for 4.5 h. Resulting supernatant (Sup) and cells (Lys) were separately collected. Western blotting for caspase-1 (casp1) or IL-1β (A, B, C and D) and ELISA for IL-1β (E and F) were performed. Representative data were shown (A, B, E and F). After densitometric analysis, relative expression of active caspase-1 was shown of three independent experiments (C and D). Dotted lines indicate control expression (Ctrl).

C). Furthermore, Nalp3$^{-/-}$ mice, like Asc$^{-/-}$ mice [29], were resistant to *P. acnes*/LPS-induced liver injury (Fig. 6D and E). Taken together these results clearly demonstrated that Nalp3 inflammasome is essential for *in vivo* release of IL-18 and the resulting liver injury.

4. Discussion

This study clearly demonstrated that MyD88 and TRIF play distinct roles in the development of liver injury after sequential treatment with *P. acnes* and LPS. MyD88 but not TRIF, presumably in hematopoietic cells [33], is essential for formation of hepatic granulomas after *P. acnes* treatment (Figs. 2 and 8). Inversely, TRIF, but not MyD88, is important for caspase-1 activation perhaps in macrophages (Figs. 4 and 8). The MyD88-dependent hepatic granuloma and the TRIF-dependent caspase-1 activation for release of IL-18 are both necessary for the serum elevated IL-18 and the development of liver injury (Fig. 2). Thus, MyD88 is essential for the priming phase, while TRIF is important for the effector phase (Fig. 8). Nalp3 inflammasome was activated during the effector phase, which eventually leading to the liver injury (Fig. 6).

Several possibilities can explain loss of the serum increase of IL-18 in *Myd88*$^{-/-}$ mice although their Kupffer cells have capacity to achieve caspase-1 activation (Fig. 4B and D). First, dense hepatic accumulation of macrophages occurs in the WT liver but not in *Myd88*$^{-/-}$ liver after *P. acnes* treatment. This is consistent with the previous report by Szabo et al. [13]. Indeed, naïve WT mice do not increase serum IL-18 or undergo liver injury after challenge with the same sublethal dose of LPS (Supplementary Fig. 2). MyD88-dependently induced chemokines and/or their receptor might be involved in accumulation of F4/80^{+} macrophages and F4/80^{-} dendritic cells [34]. Second, Kupffer cells/macrophages might proliferate after *P. acnes* treatment MyD88-dependently. Third, *Myd88*$^{-/-}$ macrophages might remain functionally premature. *Myd88*$^{-/-}$ mice poorly produce IFN-γ in response to exogenous pathogens and perhaps endogenous microbes through poor production of IFN-γ-inducing factors such as IL-12 [1]. As IFN-γ is important for priming of macrophages, *Myd88*$^{-/-}$ macrophages might not be fully activated by *P. acnes* or not become to be susceptible to following LPS. Fourth, the dose of LPS is different between*in vivo* and *in vitro* studies. We used a sublethal dose of LPS (<50 μg/kg) for *in vivo* study. Indeed, when injected with a lethal dose of LPS (>50 mg/kg), *Myd88*$^{-/-}$ mice showed elevation of serum IL-18 (Supplementary Fig. 6). Fifth, the lack of responsiveness to IL-18 in *Myd88*$^{-/-}$ mice might reduce the augmentation of IL-18 release by Fas/Fas ligand system. IL-18 induces Fas ligand, which activates macrophages to release IL-18 via activating their Fas receptor [15]. Thus, MyD88 signaling renders mice highly susceptible to LPS by numerical increase of activated macrophages. Even though they are susceptible to LPS, *P. acnes*-primed mice evade the liver injury in the absence of TRIF signalings.

Our results clearly demonstrated a critical role of the TLR4-mediated TRIF pathway for activation of Nalp3 inflammasome for caspase-1 activation (Fig. 8). Indeed, *Asc*$^{-/-}$ Kupffer cells could not complete caspase-1 activation, resulting in the absence of release both IL-18 and IL-1β (Supplementary Fig. 7). Thus, it is plausible that TRIF signaling might activate Nalp3 inflammasome. However, in spite of our intensive efforts we could not detect the association between Nalp3 protein and TRIF or between ASC and TRIF in LPS-stimulated human

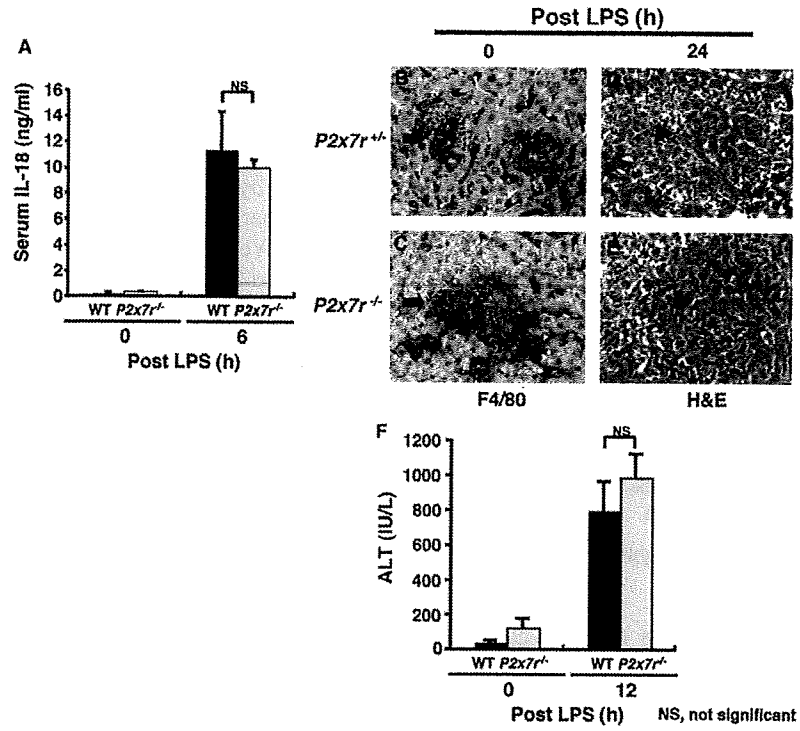

Fig. 5. Dispensability of endogenous ATP signaling for the liver injury. *P. acnes*-primed WT littermates (A and F), $P2x7r^{+/-}$ littermates (B and D) or $P2x7r^{-/-}$ mice (A, C, E and F) were challenged with LPS, and at the indicated time points sera (A and F) and liver specimens (B–E) were sampled for measurement of IL-18 concentrations (A) and ALT levels (F). F4/80$^+$ cells were determined by immunohistochemistry (B and C). Liver sections were stained by H&E (D and E). Arrows indicate hepatic granulomas, and arrowheads indicate necrotic lesion. Original magnification: 100×.

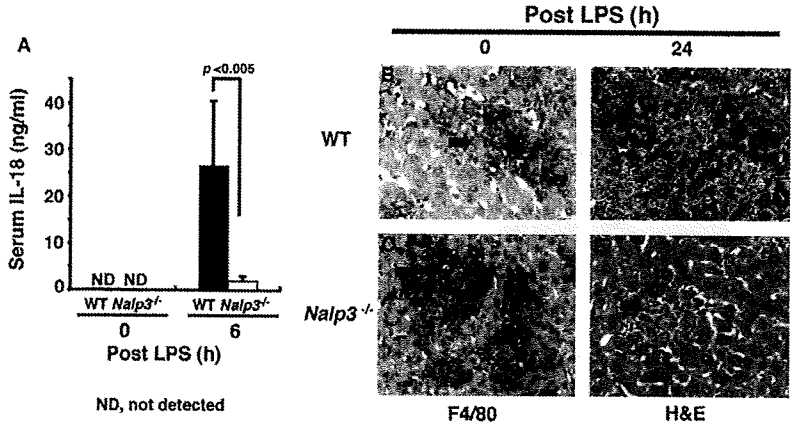

Fig. 6. Essential role for Nalp3 protein in the development of liver injury. *P. acnes*-primed WT (A, B, and D) or $Nalp3^{-/-}$ mice (A, C and E) were challenged with LPS, and at the indicated time points sera and liver specimens were sampled. Serum IL-18 concentrations (A) were measured. F4/80$^+$ cells were determined by immunohistochemistry (B and C). Liver sections were stained by H&E (D and E). Arrows indicate hepatic granulomas, and an arrowhead indicates necrotic lesion. Original magnification: 100×.

monocytic THP-1 cells or THP-1 cells that over-express TRIF, ASC and Nalp3 proteins. Therefore, although TRIF cannot interact with Nalp3 inflammasome, TRIF-mediated signal may activate Nalp3 inflammasome by induction of some mediators (cytoplasmic molecules or metabolites).

Recent reports revealed that Nalp3 inflammasome is involved in inflammatory tissue damages of several diseases. Self-derived monosodium urate crystal relevant to gouty arthritis activates Nalp3 inflammasome to release IL-1β, which eventually initiates joint inflammation [26]. Previously, we also found that murine macrophages can

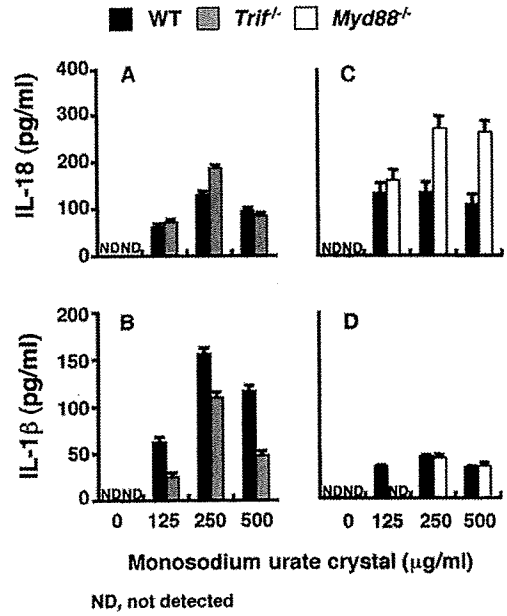

Fig. 7. Dispensability of TRIF and MyD88 for monosodium urate crystal-induced IL-18/IL-1 β secretion. WT (closed bars), $Trif^{-/-}$ (hatched bars), and $Myd88^{-/-}$ Kupffer cells (white bars) were incubated with various doses of monosodium urate crystal for 16 h. Concentrations of IL-18 (A and C) and IL-1β (B and D) were measured.

secrete both IL-18 and IL-1β in a caspase-1-dependent manner in response to monosodium urate crystal [28]. In addition to the aforementioned TRIF-mediated Nalp3 inflammasome activation, we formally succeeded in demonstrating the TRIF-independent Nalp3-dependent caspase-1 activation in Kupffer cells. $Myd88^{-/-}$ cells and $Trif^{-/-}$ Kupffer cells were able to secrete both IL-18 and IL-1β in response to monosodium urate crystal (Fig. 7). Therefore, at least two distinct signalings can activate Nalp3 inflammasome; one is TRIF-dependent pathway activated by TLR4 agonist and the other is TRIF-independent pathway initiated by monosodium urate crystal (Fig. 8). We need further study to reveal which pathway is activated by the individual inflammatory stimuli.

In summary, MyD88 and TRIF signalings play a different biological role. MyD88 is beneficial for health, such as homeostatic liver regeneration [5] and host defense [1]. As shown here, TRIF is necessary for activation of Nalp3 inflammasome for caspase-1 activation. Either single signaling could not induce liver injury. However, simultaneous or sequential activation of both signalings cause harmful outcomes (Fig. 8). Chronic inflammatory diseases with poorly identified mechanisms might be caused by the persistent activation of both MyD88 pathway and TRIF-mediated Nalp3 activation pathway.

Acknowledgements

This work was supported in part by Grants and a Hi-tec Research Center Grant from the Ministry of Education, Culture, Sports, Science and Technology of Japan, and by Grants from the Naito Foundation and the Japanese Foundation for Applied Enzymology.

We thank Dr. Kondo at Hyogo College of Medicine for enthusiastic discussion.

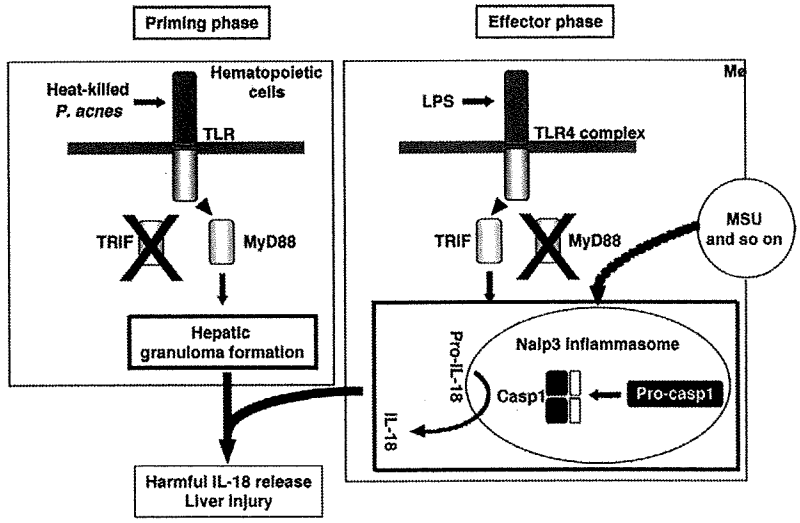

Fig. 8. A proposal model for IL-18-dependent *P. acnes*/LPS-induced liver injury. After treatment of mice with heat-killed *P. acnes*, hematopoietic cells are activated for the formation of dense hepatic granuloma consisting of many $F4/80^{+}$ cells in a MyD88-dependent but TRIF-independent manner (priming phase). LPS stimulation induces caspase-1 activation and resultant release of mature IL-18 via activating Nalp3 inflammasome in macrophages in a TRIF-dependent but MyD88-independent manner, which eventually leading to the development of liver injury (effector phase). Nalp3 inflammasome is also activated by various inflammatory stimuli, such as monosodium urate crystal (MSU), in which neither TRIF nor MyD88 are involved. Therefore, Nalp3 inflammasome is activated by at least two pathways; TLR-mediated TRIF-dependent pathway and TRIF- and MyD88-independent one.

Appendix A. Supplementary data

Supplementary data associated with this article can be found, in the online version, at doi:10.1016/j.jhep.2009.03.027.

References

[1] Akira S, Uematsu S, Takeuchi O. Pathogen recognition and innate immunity. Cell 2006;124:783–801.

[2] Seki E, Brenner DA. Toll-like receptors and adaptor molecules in liver disease: update. Hepatology 2008;48:322–335.

[3] Tsutsui H, Matsui K, Okamura H, Nakanishi K. Pathophysiological roles of interleukin-18 for inflammatory liver diseases. Immunol Rev 2000;174:192–209.

[4] Sawaki J, Tsutsui H, Hayashi N, Yasuda K, Akira S, Tanizawa T, et al. Type 1 cytokine/chemokine production by mouse NK cells following activation of their TLR/MyD88-mediated pathways. Int Immunol 2007;19:311–320.

[5] Seki E, Tsutsui H, Iimuro Y, Naka T, Son G, Akira S, et al. Contribution of Toll-like receptor/Myeloid differentiation factor 88 signaling to murine liver regeneration. Hepatology 2005;41:443–450.

[6] Campbell JS, Riehle KJ, Brooling JT, Bauer RL, Mitchell C, Fausto N. Proinflammatory cytokine production in liver regeneration is *Myd88*-dependent, but independent of *Cd14*, *Tlr2* and *Tlr4*. J Immunol 2006;176:2522–2528.

[7] Finotto S, Siebler J, Hausding M, Schipp M, Wirtz S, Klein S, et al. Severe hepatic injury in interleukin 18 transgenic mice: a key role for IL-18 in regulating hepatocyte apoptosis in vivo. Gut 2004;53:392–400.

[8] Seki E, Tsutsui H, Nakano H, Tsuji NM, Hoshino K, Adachi O, et al. LPS-induced IL-18 secretion from murine Kupffer cells independently of MyD88 that is critically involved in induction of production of IL-12 and IL-1β. J Immunol 2001;166:2651–2657.

[9] Tu Z, Bozorgzadeh A, Pierce RH, Kurtis J, Crispe NI, Orloff MS. TLR-dependent cross talk between human Kupffer cells and NK cells. J Exp Med 2008;205:233–244.

[10] Tsutsui H, Matsui K, Kawada N, Hyodo Y, Hayashi N, Okamura H, et al. IL-18 accounts for both TNF-α- and Fas ligand-mediated hepatotoxic pathways in endotoxin-induced liver injury in mice. J Immunol 1997;159:3961–3967.

[11] Sakao Y, Takeda K, Tsutsui H, Kaisho T, Nomura F, Okamura H, et al. IL-18-deficient mice are resistant to endotoxin-induced liver injury but highly susceptible to endotoxin shock. Int Immunol 1999;11:471–480.

[12] Tsuji H, Mukaida N, Harada A, Kaneko S, Matsushita E, Nakanuma Y, et al. Alleviation of lipopolysaccharide-induced acute liver injury in *Propionibacterium acnes*-primed IFN-γ-deficient mice by a concomitant reduction of TNF-α, IL-12, and IL-18 production. J Immunol 1999;162:1049–1055.

[13] Velayudham A, Hritz I, Dolganiuc A, Mondrekar P, Kurt-Jones E, Szabo G. Critical role of Toll-like receptors and the common TLR adaptor, MyD88, in induction of granulomas and liver injury. J Hepatol 2006;45:813–824.

[14] Tsutsui H, Nakanishi K, Matsui K, Higashino K, Okamura H, Miyazawa Y, et al. Interferon-γ-inducing factor up-regulates Fas ligand-mediated cytotoxic activity of murine natural killer cell clones. J Immunol 1996;157:3967–3973.

[15] Tsutsui H, Kayagaki N, Kuida K, Nakano H, Hayashi N, Takeda K, et al. Caspase-1-independent, Fas/Fas ligand-mediated IL-18 secretion from macrophages causes acute liver injury in mice. Immunity 1999;11:359–367.

[16] Nakanishi K, Yoshimoto T, Tsutsui H, Okamura H. Interleukin-18 regulates both Th1 and Th2 responses. Annu Rev Immunol 2001;19:423–474.

[17] Okamura H, Tsutsui H, Komatsu T, Yutsudo M, Hakura A, Tanimoto T, et al. Cloning of a new cytokine that induces IFN-a production by T cells. Nature 1995;378:88–91.

[18] Kuida K, Lippke JA, Ku G, Harding MW, Livingston DJ, Su MS, et al. Altered cytokine export apoptosis in mice deficient in interleukin-1® converting enzyme. Science 1995;267:2000–2003.

[19] Dinarello CA. Interleukin-1β, interleukin-18, and the interleukin-1β converting enzyme. Ann NY Acad Sci 1998;856:1–11.

[20] Gu Y, Kuida K, Tsutsui H, Ku G, Hsiao K, Fleming MA, et al. Activation of interferon-γ inducing factor mediated by interleukin-1β converting enzyme. Science 1997;275:206–209.

[21] Ghayur T, Banerjee S, Hugunin M, Butler D, Herzog L, Carter A, et al. Caspase-1 processes IFN-γ-inducing factor and regulates LPS-induced IFN-γ production. Nature 1997;386:619–623.

[22] Martinon F, Tschopp J. Inflammatory caspases and inflammasomes: master switches of inflammation. Cell Death Differ 2007;14:10–22.

[23] Neven B, Prieur AM, Quartier dit Maire PM. Cryopyrinopathies: update on pathogenesis and treatment. Nat Clin Proct Rheumatol 2008;4:481–489.

[24] Yamamoto M, Sato S, Hemmi H, Hoshino K, Kaisho T, Sanjo H, et al. Role of Adaptor TRIF in the MyD88-independent Toll-like receptor signaling pathway. Science 2003;301:640–643.

[25] Adachi O, Kawai T, Takeda K, Matsumoto M, Tsutsui H, Sakagami M, et al. Targeted disruption of the MyD88 gene results in loss of IL-1β and IL-18-mediated function. Immunity 1998;9:143–150.

[26] Martinon F, Pétrilli V, Mayor A, Tardivel A, Tschopp J. Gout-associated uric acid crystals activate the NALP3 inflammasome. Nature 2006;440:237–241.

[27] Van Rooijen N, Sanders A. Elimination, blocking, and activation of macrophages: three of a kind? J Leukoc Biol 1997;62:702–709.

[28] Inokuchi T, Moriwaki T, Tsutsui H, Yamamoto A, Takahashi S, Tsutsuimi Z, et al. Plasma interleukin (IL)-18 (interferon-gamma-inducing factor) and other inflammatory cytokines in patients with gouty arthritis and monosodium urate monohydrate crystal-induced secretion of IL-18. Cytokine 2006;33:21–27.

[29] Yamamoto M, Yaginuma K, Tsutsui H, Sagara J, Guan X, Seki E, et al. ASC is essential for LPS-induced activation of procaspase-1 independently of TLR-associated signal adapter molecules. Gene Cell 2004;9:1055–1067.

[30] Iwata A, Nishio K, Winn RK, Chi EY, Henderson WRJ, Harlan JM. A broad-spectrum caspase inhibitor attenuates allergic airway inflammation in murine asthma model. J Immunol 2003;170:3386–3391.

[31] Seki E, Kondo Y, Iimuro Y, Naka T, Son G, Kishimoto T, et al. Demonstration of cooperative contribution of MET- and EGFR-mediated STAT3 phosphorylation to liver regeneration by exogenous suppressor of cytokine signalings. J Hepatol 2007;48:237–245.

[32] Solle M, Lobasi J, Perregaux DG, Stam E, Petrushova N, Koller BH, et al. Altered cytokine production in mice lacking $P2X_7$ receptors. J Biol Chem 2001;276:125–132.

[33] Hritz I, Velayudham A, Dolganius A, Kodys K, Mandrekar P, Kur-Jones E, et al. Bone marrow-derived immune cells mediate sensitization to liver injury in a myeloid differentiation factor 88-dependent fashion. Hepatology 2008;48:1342–1347.

[34] Yoneyama H, Matsuno K, Zhang Y, Murai M, Ishikawa S, Hasegawa G, et al. Regulation by chemokines of circulating dendritic cello precursor and the formation of portal tract-associated lymphid tissue granulomatous liver disease. J Exp Med 2001;193:35–50.

nature immunology

Basophils contribute to T_H2-IgE responses *in vivo* via IL-4 production and presentation of peptide–MHC class II complexes to CD4$^+$ T cells

Tomohiro Yoshimoto[1,2], Koubun Yasuda[1,2], Hidehisa Tanaka[1,2], Masakiyo Nakahira[1,2], Yasutomo Imai[1,2], Yoshihiro Fujimori[3] & Kenji Nakanishi[1,2]

Basophils express major histocompatibility complex class II, CD80 and CD86 and produce interleukin 4 (IL-4) in various conditions. Here we show that when incubated with IL-3 and antigen or complexes of antigen and immunoglobulin E (IgE), basophils internalized, processed and presented antigen as complexes of peptide and major histocompatibility complex class II and produced IL-4. Intravenous administration of ovalbumin-pulsed basophils into naive mice 'preferentially' induced the development of naive ovalbumin-specific CD4$^+$ T cells into T helper type 2 (T_H2) cells. Mice immunized in this way, when challenged by intravenous administration of ovalbumin, promptly produced ovalbumin-specific IgG1 and IgE. Finally, intravenous administration of IgE complexes rapidly induced T_H2 cells only in the presence of endogenous basophils, which suggests that basophils are potent antigen-presenting cells that 'preferentially' augment T_H2-IgE responses by capturing IgE complex.

Atopic people, after repeated exposure to a particular antigen, develop strong T helper type 2 (T_H2) responses and produce immunoglobulin E (IgE). IgE then sensitizes mast cells and basophils by binding to their FcεRI receptor (A000543)[1–3]. Subsequent exposure to the same antigen activates the mast cells and basophils to secrete the chemical mediators, cytokines and chemokines that result in the pathological reactions of immediate hypersensitivity. IgE is a unique antibody that upregulates expression of FcεRI on mast cells and basophils, thereby providing a mechanism for the amplification of IgE-mediated reactions[4,5]. Indeed, a strong positive correlation exists between FcεRI expression on basophils and IgE titers in human peripheral blood[6]. Furthermore, as with the inhalation of ragweed pollen, low antigen dose without adjuvant can induce IgE production, which suggests that there is an amplification loop for IgE production *in vivo*. Thus, once atopic people begin to produce IgE, they develop progressive allergic inflammation by increasing production of IgE and expression of FcεRI on effector cells.

Basophils and mast cells are important effector cells in IgE-mediated allergic inflammation[1–3]. Progenitors of mast cells in the bone marrow migrate to the peripheral tissues as immature cells and undergo differentiation *in situ*[1,7]. Thus, normally, mature mast cells are not found in the circulation. In contrast, basophils are rare circulating granulocytes that originate from progenitors in the bone marrow. Basophils constitute less than 1% of blood leukocytes and are normally not present in tissues. However, they may be recruited to some inflammatory sites where antigen is present and contribute to immediate hypersensitivity reactions[8–11]. Studies also suggest that basophils induce IgE-mediated chronic allergic inflammation and IgG1-mediated systemic anaphylactic shock[12–14]. Thus, basophils are primary effector cells in allergic disorders.

However, some lines of evidence have shown that these cells are important regulators of T_H2 responses *in vivo*, particularly in helminth-infected mice[15–20]. In general, the entry of an invading pathogen triggers recognition by dendritic cells (DCs) through Toll-like receptors (TLRs) and their subsequent maturation to express costimulatory molecules and produce interleukin 12 (IL-12) and IL-18, which favor T_H1 responses[21–24]. In contrast, infection with helminths strongly induces T_H2 cells and the proliferation of basophils in the spleens and livers of host mice[18], which suggests a contribution of basophils to the induction and/or augmentation of T_H2 responses. The development of naive CD4$^+$ T cells into T_H2 cells is dependent on IL-4 (A001262) in the milieu[25]. However, the nature of cells that produce 'early' IL-4, required for the development of naive CD4$^+$ T cells into T_H2 cells, remains unknown[26]. IL-18 with IL-3 or IL-33 with IL-3 strongly induces basophils but not mast cells to produce both IL-4 and IL-13 *in vitro*[27,28], which suggests basophils are involved in the induction of T_H2 cells by functioning as early IL-4-producing cells. Other published studies have also indicated that basophils are critically involved in T_H2 responses by their unique ability to produce early IL-4 and thymic stromal lymphopoietin in response to papain or

[1]Department of Immunology and Medical Zoology, Hyogo College of Medicine, Nishinomiya, Hyogo, Japan. [2]Collaborative Development of Innovative Seeds, Japan Science and Technology Corporation, Saitama, Japan. [3]Laboratory of Cell Transplantation, Institute for Advanced Medical Sciences, Hyogo College of Medicine, Nishinomiya, Hyogo, Japan. Correspondence should be addressed to K.N. (nakaken@hyo-med.ac.jp).

Received 16 December 2008; accepted 14 April 2009; published online 24 May 2009; doi:10.1038/ni.1737

bromelain[29]. Thus, here we studied the mechanism that accounts for the induction and progression of allergic response by positive feedback loops between IgE and basophils *in vivo*. We demonstrate the contribution of basophils to the T_H2-IgE response *in vitro* and *in vivo* through the production of IL-4 and presentation of complexes of peptide and major histocompatibility complex (MHC) class II to naive $CD4^+$ T cells, in contrast to the T_H1 cell–inducing action of DCs.

RESULTS

Basophils induce the development of T_H2 cells *in vitro*

We first examined the ability of splenic basophils from naive mice and mice infected with *Strongyloides venezuelensis*[30] to produce T_H2 cytokines and to induce the development of naive $CD4^+$ cells into T_H2 cells *in vitro*. We prepared non–T cell, non–B cell fractions from spleens of naive mice and infected mice and determined the proportion of $Fc\varepsilon RI^+c\text{-}Kit^-$ cells (basophils) in those fractions. Non–T cell, non–B cell fractions from spleens of naive mice contained 0.20% $Fc\varepsilon RI^+c\text{-}Kit^-$ cells, whereas those from *S. venezuelensis*–infected mice had a much greater proportion of these cells (5.84%; **Fig. 1a**), as reported for mice infected with *Nippostrrongylus brasiliensis*[18]. Furthermore, *S. venezuelensis*–infected mice had a greater proportion of $Fc\varepsilon RI^+c\text{-}Kit^+$ cells (mast cells) in those fractions (0.02% in naive mice compared with 0.39% in infected mice). We purified basophils from the spleens of naive mice and infected mice (**Fig. 1a**) and examined their production of cytokines and expression of MHC class II molecules. Splenic basophils from infected mice cultured for 24 h with IL-3 produced large amounts of IL-4, IL-6 and IL-13, whereas those from naive mice produced small amounts of these T_H2 cytokines, although both types of basophils produced similar amounts of IL-10 (**Fig. 1b**). However, the production of IL-17A, interferon-γ (IFN-γ) and tumor necrosis factor was low (**Fig. 1b**). As reported before[27], basophils from infected mice were able to produce IL-4 without IL-3 stimulation, whereas basophils from naive mice did not produce IL-4 in the absence of IL-3 *in vitro* (**Supplementary Table 1** online), which suggests that basophils in infected mice gain the ability to produce substantial IL-4 even in the absence of IL-3. Flow cytometry of basophils from naive mice and infected mice showed that they had abundant and comparable expression of MHC class II (**Fig. 1c**). Peripheral blood basophils from naive mice also expressed MHC class II molecules (**Fig. 1c**).

As splenic basophils from infected mice expressed MHC class II and had the potential to produce substantial IL-4, IL-6 and IL-13 in cultures containing IL-3, we next examined their ability to induce ovalbumin (OVA)-specific naive $CD4^+$ T cells to develop into T_H2 cells *in vitro* in the presence of OVA peptide (amino acids 323–339 (OVA(323–339)), IL-2 and IL-3 without IL-4 ('neutral' culture conditions). We simultaneously cultured naive $CD4^+$ T cells with conventional antigen-presenting cells (APCs; T cell–depleted splenic cell samples (ΔT-spleen cells)) in the presence of OVA(323–339) in neutral conditions (**Fig. 1d**). Splenic basophils from *S. venezuelensis*–infected mice showed a notable ability to induce naive $CD4^+$ T cells to develop into T_H2 cells (**Fig. 1d**). In contrast, as reported elsewhere[25], conventional APCs failed to induce T_H2 cells in these neutral conditions, although both types of APC strongly induced the development of T_H2 cells in T_H2 conditions (**Fig. 1d**). We found that like typical T_H2 cells that developed in T_H2 conditions

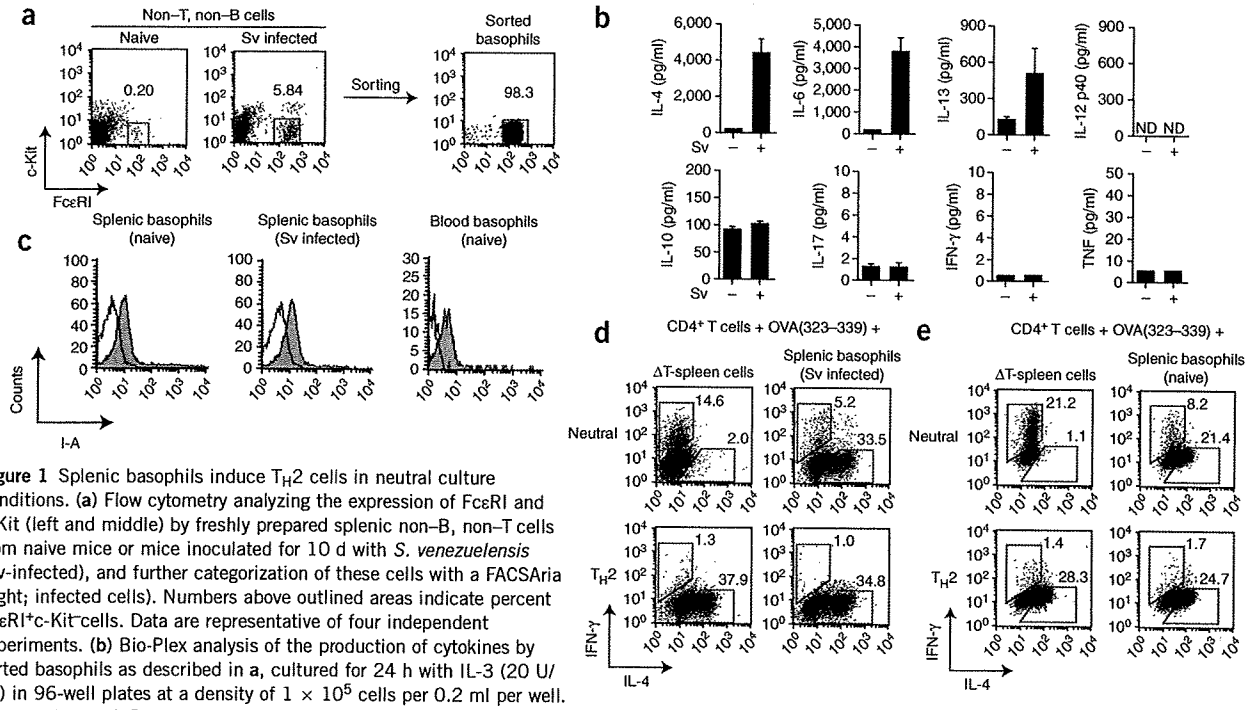

Figure 1 Splenic basophils induce T_H2 cells in neutral culture conditions. **(a)** Flow cytometry analyzing the expression of FcεRI and c-Kit (left and middle) by freshly prepared splenic non–B, non–T cells from naive mice or mice inoculated for 10 d with *S. venezuelensis* (Sv-infected), and further categorization of these cells with a FACSAria (right; infected cells). Numbers above outlined areas indicate percent $Fc\varepsilon RI^+c\text{-}Kit^-$cells. Data are representative of four independent experiments. **(b)** Bio-Plex analysis of the production of cytokines by sorted basophils as described in **a**, cultured for 24 h with IL-3 (20 U/ml) in 96-well plates at a density of 1×10^5 cells per 0.2 ml per well. ND, not detected. Data are representative of two independent experiments (mean and s.e.m. of three mice). **(c)** Flow cytometry of sorted splenic basophils from naive mice (left) or *S. venezuelensis*–infected mice (middle), stained for MHC class II molecules (I-A), and of peripheral blood mononuclear cells from naive mice, stained for MHC class II molecules and gated on $Fc\varepsilon RI^+DX5^+B220^-CD3^-$ cells (right). Filled histograms, markers; lines, unstained cells. Data are representative of two independent experiments with five mice. **(d,e)** Flow cytometry analyzing cytosolic IL-4 and IFN-γ in naive splenic DO11.10 $CD4^+CD62L^+$ T cells (1×10^5 cells per ml) stimulated for 7 d in 48-well plates with IL-2 (100 pM), IL-3 (20 U/ml) and OVA(323–339) (1 μM) in the presence of irradiated BALB/c ΔT-spleen cells or irradiated splenic basophils (5×10^5 cells per ml each) from *S. venezuelensis*–infected mice **(d)** or naive mice **(e)**, with (T_H2) or without (Neutral) IL-4 (1,000 U/ml), then washed and recultured for 4 h with the phorbol ester PMA (50 ng/ml) plus ionomycin (0.5 μg/ml). Numbers adjacent to outlined areas indicate percent $IL\text{-}4^+$ or $IFN\text{-}\gamma^+$ cells gated on $CD4^+$ T cells. Data are representative of three independent experiments.

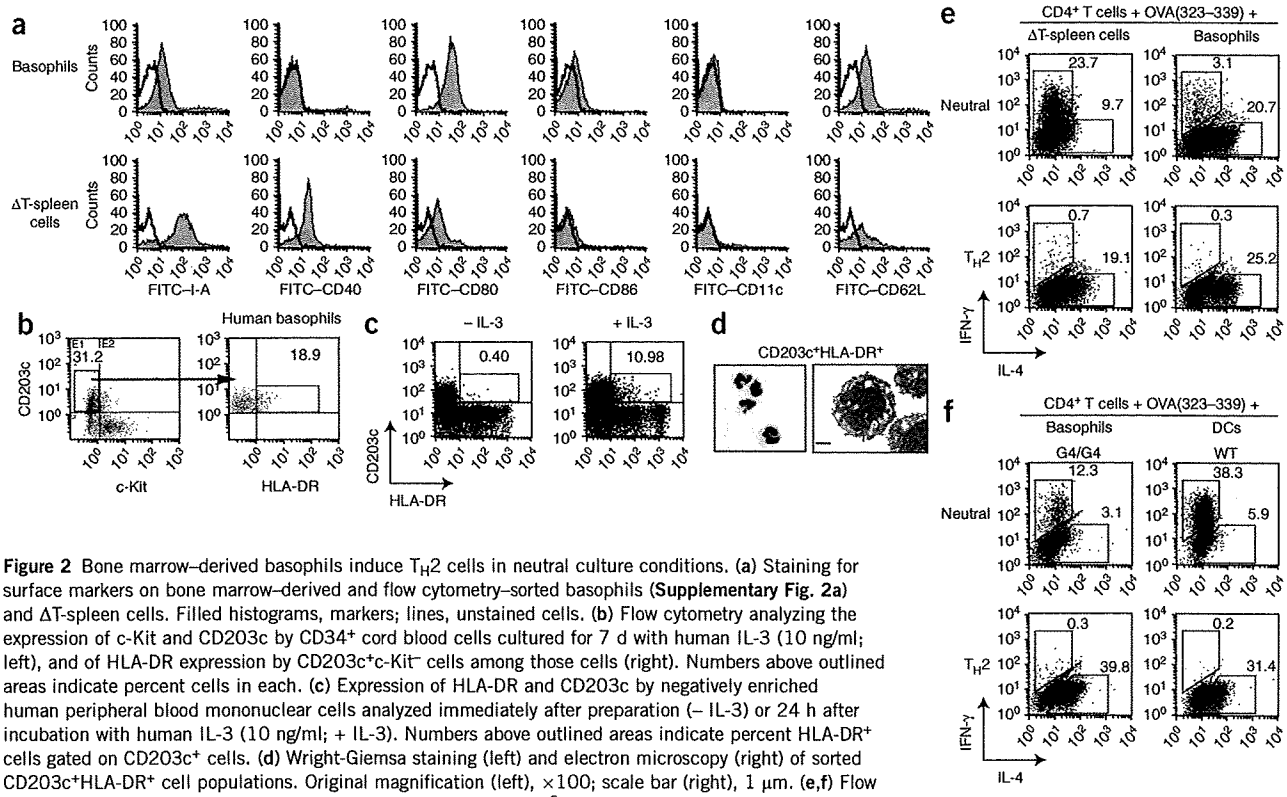

Figure 2 Bone marrow–derived basophils induce T_H2 cells in neutral culture conditions. (**a**) Staining for surface markers on bone marrow–derived and flow cytometry–sorted basophils (**Supplementary Fig. 2a**) and ΔT-spleen cells. Filled histograms, markers; lines, unstained cells. (**b**) Flow cytometry analyzing the expression of c-Kit and CD203c by $CD34^+$ cord blood cells cultured for 7 d with human IL-3 (10 ng/ml; left), and of HLA-DR expression by $CD203c^+c\text{-}Kit^-$ cells among those cells (right). Numbers above outlined areas indicate percent cells in each. (**c**) Expression of HLA-DR and CD203c by negatively enriched human peripheral blood mononuclear cells analyzed immediately after preparation (– IL-3) or 24 h after incubation with human IL-3 (10 ng/ml; + IL-3). Numbers above outlined areas indicate percent $HLA\text{-}DR^+$ cells gated on $CD203c^+$ cells. (**d**) Wright-Giemsa staining (left) and electron microscopy (right) of sorted $CD203c^+HLA\text{-}DR^+$ cell populations. Original magnification (left), ×100; scale bar (right), 1 μm. (**e,f**) Flow cytometry of naive splenic DO11.10 $CD4^+CD62L^+$ T cells (1×10^5 cells per ml) stimulated and analyzed as described in **Figure 1d**, with irradiated ΔT-spleen cells, purified bone marrow–derived wild-type (WT) or IL-4-deficient (G4/G4) basophils or wild-type splenic DCs as APCs. Data are representative of three or four independent experiments.

(**Fig. 1d**), T_H2 cells that developed after culture of naive $CD4^+$ T cells together with basophils in neutral culture conditions (**Fig. 1d**) produced IL-4, IL-5, IL-6, IL-10 and IL-13 (**Supplementary Fig. 1a** online), which suggested that these were true T_H2-polarized cells.

Next we assessed whether basophils from naive mice were also able to induce the development of T_H2 cells *in vitro*. We found that those splenic basophils also had a potent T_H2 cell–inducing function (**Fig. 1e**). As expected, some of the T_H2 cells induced in neutral conditions (**Fig. 1d**) expressed T_H2 cell marker IL-33Rα[31] (**Supplementary Fig. 1b**) and increased their production of T_H2 cytokines other than IL-4 when challenged with antigen plus IL-33 *in vitro* (**Supplementary Fig. 1c**).

Bone marrow basophils induce T_H2 cells *in vitro*

We next examined the ability of highly purified bone marrow basophils (**Supplementary Fig. 2a** online), devoid of other potential APCs, to induce T_H2 cell development *in vitro*. We first examined their expression of MHC class II molecules and the costimulatory molecules CD80 and CD86 (**Fig. 2a**). We simultaneously examined the expression of these molecules by conventional APCs. Bone marrow–derived basophils and conventional APCs expressed MHC class II, CD80 and CD86 but not CD11c. Basophils also expressed the lymph node–homing molecule CD62L, which suggested their potential to enter into lymphoid tissues[32]. As reported before[33], a fraction of human immature basophils ($CD203c^+c\text{-}Kit^-$) derived from cord blood expressed HLA-DR (18.9%; **Fig. 2b**). Although immature basophils decrease their expression of HLA-DR after maturation[33], we found mature peripheral blood basophils re-expressed HLA-DR after being cultured for 24 h with IL-3 (**Fig. 2c,d** and **Supplementary Fig. 2b**). In contrast, mouse peripheral basophils that expressed MHC class II failed to increase this expression in IL-3-containing medium (**Supplementary Fig. 2c**).

We compared the ability of conventional APCs and basophils to induce T_H2 cell development *in vitro* in neutral and T_H2 conditions (**Fig. 2e**). In the absence of any other APC, bone marrow–derived basophils were able to induce naive $CD4^+$ T cells to develop into T_H2 cells in neutral culture conditions as described above (20.7%), whereas conventional APCs induced T_H2 cells only in T_H2 conditions (**Fig. 2e**). Additional IL-4 stimulation (T_H2 conditions) resulted in an only modestly enhanced capacity of basophils to induce T_H2 cell development (25.2%; **Fig. 2e**), which suggests that bone marrow basophils produce sufficient IL-4 for maximum development of T_H2 cells. Indeed, basophils from IL-4-deficient G4/G4 mice[34] could not induce the development of T_H2 cells (3.1%) in neutral conditions (**Fig. 2f**). However, such IL-4-deficeint basophils did induce T_H2 cells in T_H2 conditions (39.8%), which allowed us to conclude that endogenous IL-4 from basophils was essential for the development of naive $CD4^+$ T cells into T_H2 cells. As reported elsewhere[25], splenic DCs induced T_H2 cells only in T_H2 cell–inducing conditions (**Fig. 2f**).

Basophils pulsed with antigen-IgE complexes are potent APCs

It was important to demonstrate the ability of basophils to take up and process OVA protein into OVA(323–339). We used 2,4-dinitrophenyl (DNP)-conjugated OVA (DNP-OVA) instead of OVA protein in this experiment and subsequent experiments, as DNP-OVA can also yield OVA(323–339) after processing. We were able to induce OVA-specific

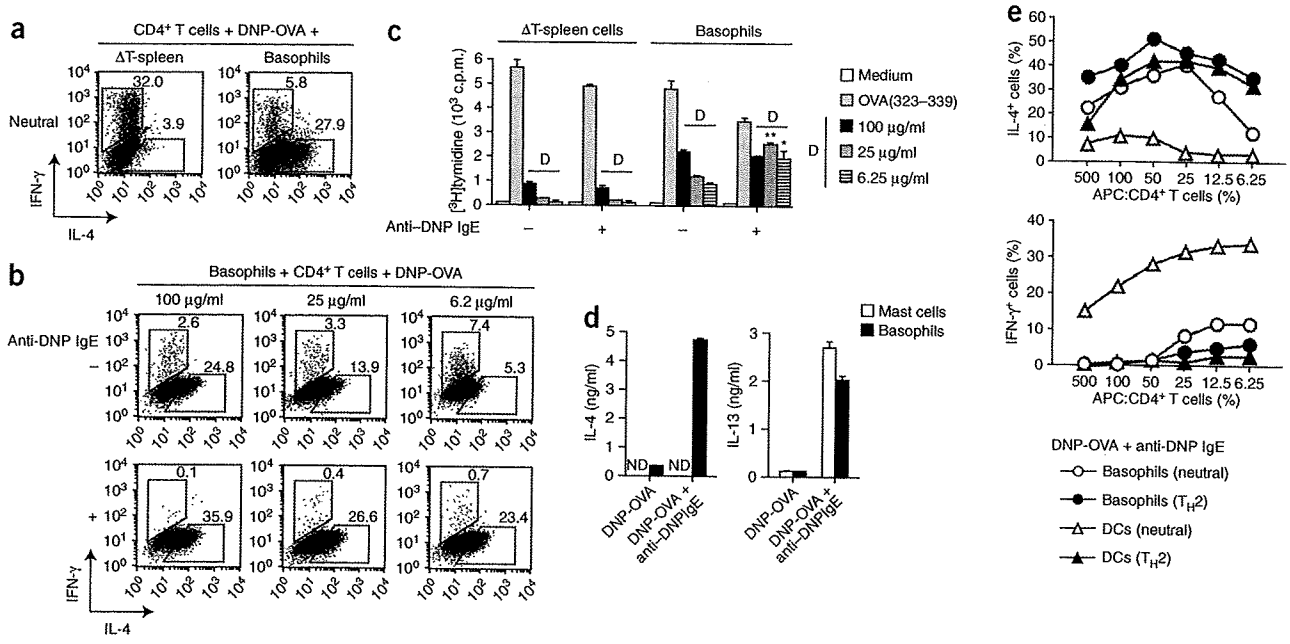

Figure 3 IgE complex enhances uptake of OVA by basophils. (**a**,**b**) Flow cytometry (as described in **Fig. 1d**) of naive splenic DO11.10 CD4$^+$CD62L$^+$ T cells (1×10^5 cells per ml) stimulated for 7 d with IL-2, IL-3 and DNP-OVA (100 μg/ml; **a**), or DNP-OVA (6.25–100 μg/ml) with or without IgE anti-DNP (10 μg/ml; **b**) in the presence of irradiated ΔT-spleen cells or bone marrow–derived basophils (5×10^5 cells per ml each). (**c**) Proliferative responses of naive splenic DO11.10 CD4$^+$CD62L$^+$ T cells (5×10^4 cells per 0.2 ml per well) cultured for 4 d in 96-well plates with OVA(323–339) (1 μM) or DNP-OVA (D; 6.25–100 μg/ml; in key) with or without IgE anti-DNP (10 μg/ml). *, $P < 0.05$ and **, $P < 0.005$, versus cells without anti–DNP IgE (Student's *t*-test). (**d**) Cytokine production by bone marrow–derived basophils or mast cells (5×10^5 cells per ml each) stimulated for 16 h in 48-well plates with IL-3 and DNP-OVA (100 μg/ml) with or without IgE anti-DNP (10 μg/ml). (**e**) Flow cytometry (as described in **Fig. 1d**) of naive splenic DO11.10 CD4$^+$CD62L$^+$ T cells (1×10^5 cells per ml) stimulated for 7 d with IL-2, IL-3, DNP-OVA (100 μg /ml) and IgE anti-DNP (10 μg /ml) in the presence of various numbers (6.25×10^3 to 5×10^5 cells per ml) of irradiated splenic DCs or bone marrow basophils with IL-4 (T_H2) or without IL-4 (Neutral). Data are representative of four (**a**–**d**) or two (**e**) independent experiments (mean and s.e.m. in **c**,**d**).

T_H2 cells by culturing naive CD4$^+$ T cells with basophils in the presence of IL-2, IL-3 and DNP-OVA (100 μg/ml) without IL-4 (**Fig. 3a**). Again, conventional APCs failed to induce the development of T_H2 cell in these neutral culture conditions (**Fig. 3a**). Thus, basophils are able to process DNP-OVA into OVA(323–339) and to display peptide fragment in association with MHC class II and to produce IL-4.

It was also important to demonstrate the unique potential of basophils to increase their capacity to act as APCs when pulsed with antigen in the presence of antigen-specific IgE. Thus, we pulsed basophils with various doses of DNP-OVA in the presence or absence of monoclonal antibody to DNP (IgE anti-DNP; **Fig. 3b**). Basophils pulsed with a low dose (6.2 μg/ml) of DNP-OVA modestly induced T_H2 cells (5.3%), whereas pulsation with a higher dose (100 μg/ml) of DNP-OVA resulted in a higher proportion of 24.8%. The addition of IgE anti-DNP resulted in much higher proportions, particularly at lower concentrations of DNP-OVA (no IgE anti-DNP, 5.3%, 13.9% and 24.8%, versus with IgE anti-DNP, 23.4% 26.6% and 35.9%, for 6.2 μg/ml, 25 μg/ml and 100 μg/ml of DNP-OVA, respectively; **Fig. 3b**). Thus, the enhancing effect of IgE anti-DNP on basophil-induced T_H2 cell development was most apparent when basophils were pulsed with low concentrations of DNP-OVA.

We next examined whether IgE anti-DNP could enhance the capacity of conventional APCs to function as APCs. Thus, we cultured OVA(323–339)-specific T cells with conventional APCs or basophils in the presence of OVA(323–339) or DNP-OVA with or without IgE anti-DNP. Basophils pulsed with DNP-OVA in the presence of IgE anti-DNP had a significantly greater capacity to induce the proliferation of OVA–specific T cells (**Fig. 3c**). In contrast, conventional APCs pulsed with DNP-OVA in the presence of IgE anti-DNP did not have a greater capacity to induce T cell proliferation (**Fig. 3c**). These results suggest that basophils, taking advantage of their expression of FcεRI, might efficiently take up low doses of antigen in an IgE-dependent way.

As reported before[35], basophils had a much greater capacity to produce IL-4 and IL-13 after being pulsed with DNP-OVA in the presence of IgE anti-DNP (**Fig. 3d**). In contrast, mast cells pulsed with DNP-OVA–IgE anti-DNP immune complexes produced only IL-13, not IL-4 (**Fig. 3d**). We prepared basophils and mast cells from bone marrow cells cultured for 14 d with IL-3 (**Supplementary Fig. 2a**). We stimulated those cells with mixture of DNP-OVA and IgE anti-DNP. Mast cells prepared from bone marrow cells cultured for 4–6 weeks in medium conditioned by mouse leukemic WEHI-3 cells (containing IL-3) are reported to produce IL-4 after sequential IgE anti-DNP sensitization and subsequent DNP-protein challenge[36]. In addition to that unique function, we found that only basophils, when stimulated with IL-3 plus IL-18, IL-33, peptidoglycan or lipopolysaccharide, produced both IL-4 and IL-13 (**Supplementary Fig. 3a,b** online). Thus, basophils became producers of large amounts of IL-4 in *S. venezuelensis*–infected mice (**Fig. 1b**) or *in vitro* when stimulated with DNP-OVA–anti-DNP IgE in the presence of IL-3. Next we compared the APC activity of basophils and sorted CD11c$^+$ splenic DCs[37] by changing the ratio of APCs to naive CD4$^+$ T cells. Again, only basophils 'preferentially' induced the development of T_H2 cells in